Evolution of Debris Disks

Mark C. Wyatt

Institute of Astronomy, University of Cambridge, Cambridge CB3 0HA, United Kingdom;
email: wyatt@ast.cam.ac.uk

Key Words

circumstellar disks, extrasolar planetary systems, main sequence stars,
planet formation, Solar System

Abstract

Circumstellar dust exists around several hundred main sequence stars. For
the youngest stars, that dust could be a remnant of the protoplanetary disk.
Mostly it is inferred to be continuously replenished through collisions be-
tween planetesimals in belts analogous to the Solar System's asteroid and
Kuiper belts, or in collisions between growing protoplanets. The evolution
of a star's debris disk is indicative of the evolution of its planetesimal belts
and may be influenced by planet formation processes, which can continue
throughout the first gigayear as the planetary system settles to a stable con-
figuration and planets form at large radii. Evidence for that evolution comes
from infrared photometry of large numbers of debris disks, providing snap-
shots of the dust present at different evolutionary phases, as well as from
images of debris disk structure. This review describes the theoretical frame-
work within which debris disk evolution takes place and shows how that
framework has been constrained by observations.

1. INTRODUCTION

The Solar System is comprised not just of planets, but also numerous smaller objects ranging from those 2000 km in diameter such as Pluto and Eris, down to submicrometer-sized dust. Everything in the Solar System except its eight planets I will refer to as its debris disk, and this is concentrated in two belts, the asteroid belt at 2–3.5 AU and the Kuiper belt at 30–48 AU. It is such an integral part of the Solar System that there is a debate as to how to differentiate between a planet and a large member of the debris disk (Basri & Brown 2006). This was resolved recently by the International Astronomical Union, which placed the largest members of the asteroid and Kuiper belts in the dwarf planet category.

The Solar System's debris disk has not always looked as we see it today. Both the asteroid belt and the Kuiper belt are believed to have started off with considerably more mass than their current retinue (Stern 1996; O'Brien, Morbidelli & Bottke 2007, and references therein), and even the radial location of the belts may have changed over time (Gomes et al. 2005, Thommes et al. 2007). The Solar System's history is also thought to have been punctuated by events that significantly changed the local debris population, such as collisions between protoplanets or asteroids (Nesvorný et al. 2003, Canup 2004). Evidence for this evolution comes from a variety of sources: the orbits of the planets (Tsiganis et al. 2005), the size distribution and dynamical structure of the debris belts (Bottke et al. 2005; Morbidelli, Levison & Gomes 2008), the cratering records and geochemical composition of planets and debris (Halliday & Kleine 2006), and deep sea sediments on the Earth (Farley et al. 2006). Despite this evidence, the evolution of the Solar System's debris disk is still hotly debated, particularly within the first gigayear, during which the planetary system may still have been undergoing the last stages of accretion and was settling to its final configuration. The study of the Solar System's debris disk is instrumental in piecing together the events that lead to its formation and subsequent evolution (see, e.g., Lissauer 1993).

Some extrasolar systems are also known to harbor debris disks. The first extrasolar debris disk was discovered by the Infrared Astronomical Satellite (IRAS) from the thermal emission of dust heated by the star Vega (Aumann et al. 1984), and it soon transpired that several hundred nearby stars also had such a dust population (e.g., Oudmaijer et al. 1992, Mannings & Barlow 1998), including β Pictoris for which images of starlight scattered by the dust showed it to have a disk-like morphology (Smith & Terrile 1984). Much in the same way the asteroids and comets in the Solar System feed the zodiacal cloud (Mann et al. 2006), the dust seen around stars like Vega and β Pictoris must be continually replenished from a population of larger planetesimals (Backman & Paresce 1993). However, they are not typically direct analogs to the zodiacal cloud, because the inner tens of AU of extrasolar debris disks are relatively clear of dust. Rather, they are often considered to be analogs to the Solar System's Kuiper belt (Moro-Martín et al. 2008), with the proviso that the known extrasolar debris disks are necessarily an order of magnitude more massive than our own, because present instrumentation cannot yet detect dust in our current Kuiper belt.

For a long time debris disk studies were dominated by β Pictoris (Artymowicz 1997), because this was the only example that could be resolved. However, the past decade has seen growth in observational capabilities at all wavelengths from optical to millimeter, which has lead to the discovery of 20 imaged disks (Holland et al. 1998), half of which were imaged for the first time in the past two years (e.g., Kalas et al. 2007). Just as the dynamical structure of the Kuiper belt is indicative of the Solar System's history, the detailed morphology of imaged disks can be used to infer the past history of their systems (Augereau et al. 2001, Wyatt 2003, Su et al. 2005), and may even show morphological changes on decadal timescales (Poulton, Greaves & Cameron 2006).

Significant progress in our understanding of debris disk evolution since the last review of this topic in the *Annual Review of Astronomy and Astrophysics* (Zuckerman 2001) has been made possible not just by an increase in the number of imaged disks, but also by the development of methods to assign ages to nearby stars both systematically and with increasing accuracy (e.g., Zuckerman & Song 2004). This means that the growing number of known but not necessarily resolved debris disks, which provide snapshots of the debris present at a range of different evolutionary stages, allow us to piece together the evolutionary sequence that follows the 10-Myr-long protoplanetary disk phase during which most planet formation processes occur. The Infrared Space Observatory (ISO) debris disk studies were the first to benefit from systematic stellar age dating (Habing et al. 2001), allowing the dependence of the fall-off of dust mass with time originally inferred from the relatively few well-studied systems (Zuckerman & Becklin 1993, Holland et al. 1998) to be well characterized (Spangler et al. 2001), but also showing that bright debris disks persist up to several gigayears (Decin et al. 2003). These statistics have been reinforced by submillimeter studies (Najita & Williams 2005) and a reevaluation of the IRAS discoveries (Moór et al. 2006; Rhee et al. 2007), spawning a proliferation of models for debris disk evolution that have allowed researchers to interpret the observations either as protoplanetary disk remnants (Klahr & Lin 2001), or in terms of planet formation processes (Kenyon & Bromley 2004a) or internal steady-state processes (Dominik & Decin 2003).

The potential of debris disk evolution studies is now being realized with the *Spitzer Space Telescope* (*Spitzer*; Werner et al. 2004), which is sensitive to much lower levels of dust mass than its predecessors, and which is significantly increasing the complement of known debris disks. The results of the *Spitzer* debris disk surveys have been coming out over the past three years. They permit a quantitative appraisal of the different models, as well as provide a context within which to assess the ubiquity of the evolution that lead to a planetary system that, like the Solar System, is capable of sustaining life (Meyer et al. 2007). This review seeks to consolidate our understanding of debris disk evolution by outlining the theoretical framework within which debris disk evolution takes place, both from the point of view of how a debris disk is born (Section 3) and how it subsequently evolves (Section 4), and by presenting the debris disk observations and discussing their interpretation in the context of that theoretical framework (Section 5). First, though, it is important to identify the fundamental properties of a debris disk, so that the models can be presented in a manner that facilitates comparison with the observations (Section 2).

2. DEBRIS DISK FUNDAMENTALS

In the absence of detailed imaging, the majority of information about a star's debris disk (or lack thereof) is derived from the star's spectral energy distribution (SED), which includes emission from nearby dust heated by the star. Typically that information comes in the form of photometric fluxes at one or more wavelength. Given the sparse information available for most stars it is important to interpret it using a model having the fewest possible free parameters. Because the SED of known debris disks can, to a reasonable approximation, be described by a black body at a single temperature (Chen et al. 2006, Hillenbrand et al. 2008), debris disks are amenable to such simplification using a model with two free parameters.

2.1. Dust Temperature and Fractional Luminosity

The two fundamental observable parameters of a debris disk are temperature T and fractional luminosity, f, which is defined as the ratio of infrared luminosity from the dust to that of the star $f = L_{ir}/L_\star$. This is illustrated in **Figure 1a**, which shows the shape of the total emission spectrum for various levels of f and T.
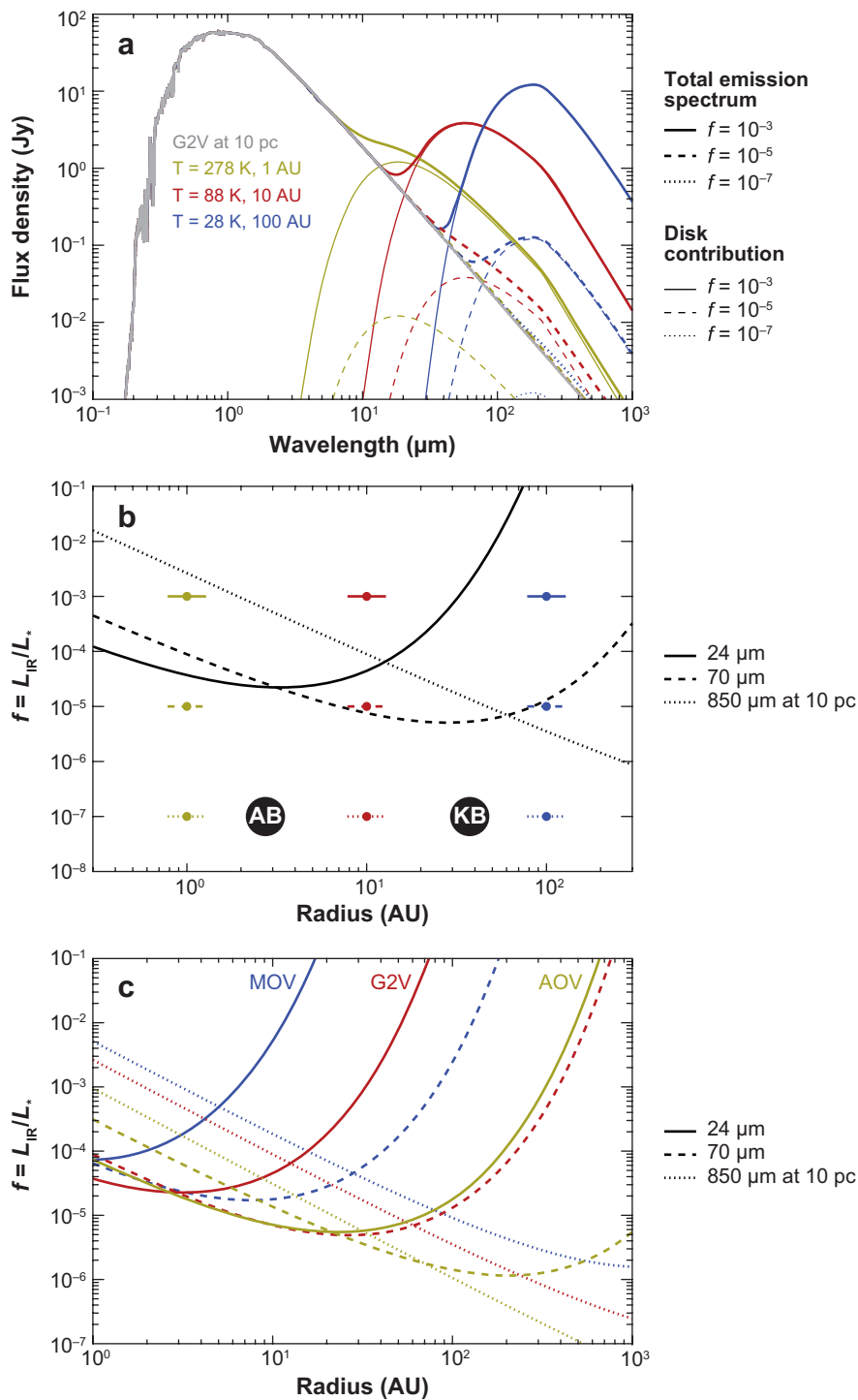
A useful rule of thumb is that these two parameters can be estimated from the wavelength and flux of the maxima in the emission spectra of the disk and of the star:

$$T = 5100/\lambda_{\text{disk, max}}, \tag{1}$$

$$f = (F_{\nu \text{ disk, max}}/F_{\nu\star, \text{ max}})(\lambda_{\star, \text{ max}}/\lambda_{\text{disk, max}}), \tag{2}$$

where λ is in micrometers and T in Kelvins. Although debris disk temperatures range from 10 K up to a few hundred K, a defining property of a debris disk is that it has a fractional luminosity $f < 10^{-2}$ (Lagrange et al. 2000), in contrast to protoplanetary disks, which have higher fractional luminosities (see Section 3.1).

2.2. Age

The question of how debris disks evolve is essentially asking how the two fundamental parameters f and T vary with stellar age. Evolution in these fundamental parameters for any one disk is not expected even on decadal timescales, although the persistence of emission from the epoch of IRAS (1983) to *Spitzer* (~2005) is a valuable constraint (e.g., Lisse et al. 2008). Thus, evolution is assessed by looking at how the distributions of fractional luminosity and dust temperature vary with age.

An understanding of stellar ages is fundamental to evolutionary studies. This review does not discuss how stellar ages are derived (see Zuckerman & Song 2004), except to note that there are several different diagnostics that can give conflicting results (e.g., Moór et al. 2006). Although insecure age determinations may affect the interpretation of individual sources, conclusions about disk evolution based on large numbers of stars are expected to be valid as long as ages are derived in a consistent manner, because relative ages can be established more accurately (e.g., Rieke et al. 2005). The discovery of young stellar associations near the Sun (Zuckerman & Song 2004) has also improved the accuracy of age determination for this subset of stars. A twist on the uncertainty in age determination is that the presence of a bright debris disk can be used to help constrain the age (Kalas et al. 2007), because a disk with $f > 0.5 - 1 \times 10^{-3}$ implies an age of <100 Myr (Zuckerman & Song 2004, Moór et al. 2006).

←——

Figure 1

Two parameter debris disk model. (*a*) Emission spectrum of a G2V star at 10 pc with a debris disk comprised of dust at temperatures of 278 K, 88 K, and 28 K shown in yellow, red, and blue, which for black body grains corresponds to radii of 1 AU, 10 AU, and 100 AU, respectively. The debris disk spectrum has been added at a level of $f = 10^{-3}$, 10^{-5}, and 10^{-7}, shown with solid, dashed, and dotted lines, respectively. The thick lines show the total emission spectrum, whereas the thin lines show the contribution of the disk. (*b*) Detection limits for 24-μm (*solid line*), 70-μm (*dashed line*), and 850-μm (*dotted line*) observations. To be detected at these wavelengths, a disk must lie above these lines. The 24- and 70-μm observations are assumed to be calibration-limited at $R_{\nu \text{ lim}} = 0.1$ and $R_{\nu \text{ lim}} = 0.55$, respectively, whereas the 850-μm observations are assumed to be sensitivity-limited at $F_{\nu \text{ lim}} = 2$ mJy, and the limit is shown for a star at 10 pc. The disks shown in the emission spectrum (*a*) are indicated with filled circles (and the same color and line styles), along with the asteroid belt (AB) and Kuiper belt (KB). The detectability of a debris disk is a strong function of both its radius and the wavelength of observation, although it should be noted that the *x* axis more specifically refers to disk temperature, which has been converted to radius using Equation 3. Observations are not yet capable of detecting the Solar System's debris disk around another star. (*c*) Same as panel b, but showing the detection limits for M0V, G2V, and A0V stars in blue, red, and yellow, respectively.

2.3. Disk Radius and Mass

To interpret the observable parameters in a way more relevant to disk evolution models, the dust is assumed to be uniformly distributed in a torus of radius r and width dr with a vertical opening angle of $2I$. The low fractional luminosity of debris disks means that they are optically thin to stellar radiation; the geometrical optical depth perpendicular to the disk plane is $f(2r/dr)$, whereas the optical depth from the star to the disk's outer edge is f/I. This means that dust temperature depends only on its distance from the star (rather than on the disk density). For heuristic purposes the dust is assumed here to behave like a black body, giving

$$r = (278.3/T)^2 L_\star^{0.5}, \qquad (3)$$

where $L_\star$ is the Sun's luminosity (equal to 3.85×10^{26} W), T is in Kelvins, and r is in astronomical units.

With these assumptions, the fractional luminosity defines the total cross-sectional area of dust in the disk,

$$\sigma_{\rm tot} = 4\pi r^2 f, \qquad (4)$$

where $\sigma_{\rm tot}$ is in AU^2. Although this can be converted into an estimate of dust mass by assuming all dust has a diameter D and density ρ (i.e., $M_{\rm tot} = 0.67\rho D\sigma_{\rm tot}$), dust masses are more typically derived directly from the disk flux (Beckwith et al. 2000),

$$M_{\rm disk} = 4.25 \times 10^{10} F_{\nu\,\rm disk} d^2 \kappa_\nu^{-1} [B_\nu(\lambda, T)]^{-1}, \qquad (5)$$

where $M_{\rm disk}$ is the mass of the Earth (equal to 5.97×10^{24} kg), $F_{\nu\,\rm disk}$ is in janskies, d is stellar distance in parsecs, and κ_ν is in $AU^2\ M_\oplus^{-1}$. In this review it is consistently assumed that $\kappa_\nu = 45$ $AU^2\ M_\oplus^{-1}$ (i.e., 0.17 m^2 kg^{-1}) for 850-μm observations, which are sensitive to millimeter- to centimeter-sized dust.

Disk flux in this model is given by

$$F_{\nu\,\rm disk} = 2.95 \times 10^{-10} B_\nu(\lambda, T) f r^2 d^{-2} X_\lambda^{-1}, \qquad (6)$$

where the factor X_λ is included to account for the falloff in the emission spectrum beyond $\sim$200 μm, which is faster than black body by an additional factor $\propto \lambda^{-1}$ (Williams & Andrews 2006). Comparison with submillimeter observations shows that $X_{850} \approx 4$ (Wyatt et al. 2007b), and **Figure 1** assumes that $X_\lambda = 1$ for $\lambda < 210$ μm and $X_\lambda = \lambda/210$ for $\lambda > 210$ μm, however the wavelength of the break and the slope of the falloff vary between disks. Equation 6 indicates that disk mass quoted using Equation 5 is a scaled version of the fractional luminosity,

$$M_{\rm disk} = 12.6 f r^2 \kappa_\nu^{-1} X_\lambda^{-1}. \qquad (7)$$

The relation $M_{\rm disk}/f \propto r^2$ has been shown to hold well across submillimeter and far-IR surveys (Rhee et al. 2007).

2.4. Calibration- and Sensitivity-Limited Surveys

Most stars exhibit no evidence of excess emission from dust, indicating that the fractional luminosities and temperatures of their debris disks are not known. The implications of a nondetection are evident from Equation 6. The fractional luminosity of a disk that is not detected to a sensitivity of $F_{\nu\,\rm lim}$ must lie below

$$f_{\rm det} = 3.4 \times 10^9 F_{\nu\,\rm lim} d^2 r^{-2} [B_\nu(\lambda, T)]^{-1} X_\lambda. \qquad (8)$$

In other words, the limit is strongly temperature (or equivalently radius) dependent, and the consequence of a nondetection is to demark a region of f versus T parameter space where the disk must lie to have escaped detection. Likewise, a detection at just one wavelength does not unambiguously constrain both f and T, but defines a locus on which f and T could lie. This is illustrated in **Figure 1*b***, which shows the limits on fractional luminosity for 24-μm, 70-μm, and 850-μm observations of a sun-like star at 10 pc that have a sensitivity of 34, 22, and 2 mJy, respectively. The debris disk of the Solar System is two orders of magnitude too faint to be detected by such observations.

Surveys generally fall into two categories, sensitivity-limited and calibration-limited. A sensitivity-limited survey can detect disks to a level described by Equation 8. The sensitivity could be limited by observing time or background confusion (either cirrus or extragalactic). A calibration-limited survey can detect disks to a level that depends on the excess ratio (also called fractional excess), $R_\nu = F_{\nu\,\mathrm{disk}}/F_{\nu\star}$. Because stellar flux is given by

$$F_{\nu\star} = 1.77 B_\nu(\lambda, T_\star) L_\star T_\star^{-4} d^{-2}, \tag{9}$$

where $T_\star$ is in Kelvins, Equation 6 gives the excess ratio as

$$R_\nu = 1.67 \times 10^{-10} B_\nu(\lambda, T)[B_\nu(\lambda, T_\star)]^{-1} f r^2 T_\star^4 L_\star^{-1} X_\lambda^{-1}. \tag{10}$$

For a calibration-limited survey a disk is detectable as long as $F_{\nu\,\mathrm{disk}}/F_{\nu\star} > R_{\nu\,\mathrm{lim}}$, so the corresponding limit on fractional luminosity is

$$f_{\mathrm{det}} = 6.0 \times 10^9 R_{\nu\,\mathrm{lim}} r^{-2} L_\star T_\star^{-4} B_\nu(\lambda, T_\star)[B_\nu(\lambda, T)]^{-1} X_\lambda. \tag{11}$$

The calibration limit could arise from uncertainties in the instrumental calibration, as well as uncertainties in contribution from stellar photospheric emission.

The thresholds appropriate for many of the *Spitzer* and the Submillimetre Common-User Bolometer Array (SCUBA) surveys discussed in this review are shown on **Figure 1*c*** for sun-like stars, as well as for main-sequence M0 and A0-type stars. Most of the *Spitzer* surveys are calibration-limited, whereas the SCUBA surveys are sensitivity-limited. It is important to keep **Figure 1** in mind when considering the observational results, because surveys of different spectral types and at different wavelengths are sensitive to different regions of parameter space, and are therefore subject to an inherent bias.

2.5. Caveats

The two-parameter model discussed here does not always provide an accurate description of the SED that for some disks can only be explained by the presence of dust at multiple temperatures (e.g., Chen et al. 2006, Hillenbrand et al. 2008). This temperature range could arise because dust is at a range of distances from the star, or because dust at the same distance from the star has a range of temperatures (Matthews, Kalas & Wyatt 2007). High-resolution imaging is required to determine which interpretation is correct. Such images show that some systems with multiple temperatures, like η Corvi, are comprised of dust at two or more radii separated by more than an order of magnitude in radius (Wyatt et al. 2005; Smith, Wyatt & Dent 2008). Most images, however, show radially confined rings (Greaves et al. 2005; Kalas, Graham & Clampin 2005), even if scattered-light imaging suggests that the rings can be broad (Kalas et al. 2006). But the number of systems, like Vega and τ Ceti, where dust has been observed using different techniques over several orders of magnitude in radius is steadily growing (Greaves et al. 2004b, Su et al. 2005, Absil et al. 2006, di Folco et al. 2007). However, the SEDs of such systems still often resemble a single-temperature black body, because much of the close-in and distant dust contributes little to

the total infrared luminosity. The nature of such systems is discussed in this review, although the dominant structure of debris disks is considered to be ring-like.

Only the largest grains in a debris disk are expected to emit light like black bodies. Dust in debris disks has a range of sizes and each size has different emission properties. This has consequences for the shape of the SED and the equilibrium temperature of the dust (Backman & Paresce 1993), and dynamical considerations show that different grain sizes may be expected to have different spatial distributions (Augereau et al. 2001; Augereau & Beust 2006; Strubbe & Chiang 2006; Wyatt 2006, 2008). Although a more realistic model for the optical properties and size distribution of the dust is readily attainable (e.g., Wyatt & Dent 2002), this review interprets the debris disk results within the context of the simple model of Sections 2.1–2.4, because differences between the simple model and the real world should affect most disks in a systematic manner. Two of these systematic differences are particularly noteworthy. The radius derived from Equation 3 can underestimate the true radius by a factor of ∼3 (e.g., Schneider et al. 2006), so although it is appropriate to compare the disk radii using this parameter, it is only a guideline to the true radius. Likewise, the disk mass given by Equations 5 and 7 depends on the assumed opacity and may not bear much resemblance to the total disk mass that could be present in large objects that contribute little to the observed emission (i.e., more than a few tens of centimeters, see figure 5 of Wyatt & Dent 2002). Nevertheless, it is instructive to compare disk masses derived with the same opacity assumptions.

3. BIRTH OF A DEBRIS DISK

Although the debris disk phenomenon as described in Section 2 is attributed to circumstellar dust, it is inferred that there must also be a belt of larger objects (planetesimals) coincident with the dust, as well as some mechanism operating to turn them into dust (e.g., Backman & Paresce 1993). For many debris disk studies, it is unnecessary to consider how the planetesimal belt came into existence. However, planet formation is thought to be a dynamic process that is ongoing throughout the first gigayear of a star's life, and one of the emerging realizations of the past few years is the extent to which the debris disk phenomenon is affected by planet formation processes, and therefore the extent to which observations of debris disks can set constraints on those processes. It has also been suggested that some debris disks are remnants of the protoplanetary disk. This section outlines the aspects of protoplanetary disk evolution and of the planetesimal and planet formation processes that are pertinent to our understanding of how debris disks are born and how they evolve.

3.1. Protoplanetary Disk Evolution

Most stars are born with disks known as protoplanetary disks (Haisch, Lada & Lada 2001). The planetesimals that feed debris disks, as well as extrasolar planets, are thought to form within protoplanetary disks, which are comprised (by mass) mainly of gas with a ∼1% contribution from dust, most of which starts off in submicrometer size (Dullemond et al. 2007). Submillimeter observations show that protoplanetary disks have a broad distribution of dust masses, which for the class II disks of sun-like stars in Taurus-Auriga and Ophiuchus is Gaussian in $\log M_{disk}$ with a mean of 30 $M_{\oplus}$ (using the fiducial opacity of Section 2.3) and a standard deviation of 0.8 dex (Andrews & Williams 2005, 2007). A broad distribution of outer gas disk radii from 10–1000 AU at all ages is also inferred from CO linewidths (Dent, Greaves & Coulson 2005). There is little evidence for evolution in the dust mass distribution with age while the disks persist (Andrews & Williams 2007), although the near-IR excess ratio, indicative of dust ≪1 AU, is seen to decrease
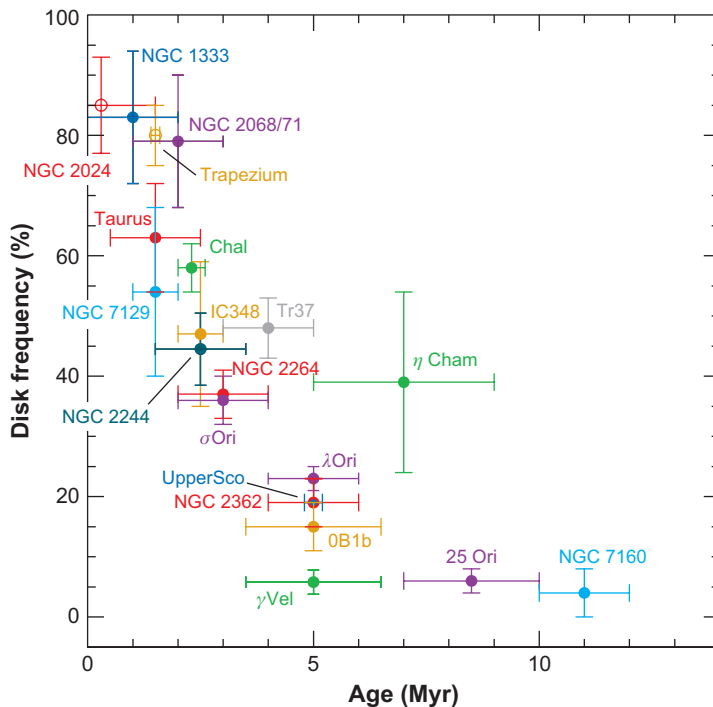
Figure 2

Evolution of protoplanetary disks—fraction of sun-like stars with detectable near-IR excess as a function of time (Hernández et al. 2007b; J. Hernández, private communication). Protoplanetary disks have a range of lifetimes, and most sun-like stars have lost their disks by 6 Myr.

with age (Carpenter et al. 2006, Hernández et al. 2007a), as is accretion of gas onto the star (Calvet et al. 2005a).

The fraction of sun-like stars with near-IR disk emission decreases from ∼100% to 0% over 6 Myr (Haisch, Lada & Lada 2001; Hernández et al. 2007b; see **Figure 2**), implying that such disks have a range of lifetimes from 1–6 Myr (Meyer et al. 2007). The protoplanetary disks of more massive stars have shorter lifetimes than those of sun-like stars, because few A stars have protoplanetary disks by 3–5 Myr (Carpenter et al. 2006, Hernández et al. 2007b); conversely, later spectral types are more likely to host protoplanetary disks at later times (Young et al. 2004, Low et al. 2005, Megeath et al. 2005, Scholz et al. 2007). Although near-IR observations probe the inner ≪1 AU of the dust disk, this dust is thought to have been dragged in by gaseous accretion disk processes, and its disappearance is usually considered to be synonymous with the disappearance of the gas, although the correspondence of accreting gas and near-IR excess is not so strict (e.g., Lada et al. 2006).

The process of protoplanetary disk dispersal is rapid compared with the stellar lifetime, because very few stars are observed having intermediate levels of near-IR excess. However, some stars without near-IR excess (from dust at ≪1 AU) still possess mid-IR excess (from dust at a few astronomical units) (e.g., McCabe et al. 2006), and a new paradigm is being forged that envisages the disks cleared from the inside-out (Calvet et al. 2005b). Even so, just 10% of disk-bearing stars are seen in a transitional phase (Sicilia-Aguilar et al. 2006, Cieza et al. 2007, Hernández et al. 2007a), illustrating the pace of the clearing process. The rapid change in disk properties at

a few million years can be reproduced by the UV switch model in which the inner disk is cleared by viscous accretion once photoevaporation at 5–10 AU prevents replenishment from the outer disk (Clarke, Gendrin & Sotomayer 2001; Alexander, Clarke & Pringle 2006). However, further observational evidence on this transition is needed before its origin is truly understood, which could alternatively be related to the formation of planets in the disk (Quillen et al. 2004).

One practical reason this transition is relevant for debris disk studies is that our understanding of the birth of debris disks derives from studies of star-forming regions where there may be a mixture of protoplanetary, transitional, and debris disks. Methods based on near-IR and mid-IR excess ratios are employed to distinguish between different disk categories, typically classifying debris disks as having 24-μm excess ratios $R_{\nu\,lim} < 100$ (e.g., Sicilia-Aguilar et al. 2006, Hernández et al. 2007b, Uzpen et al. 2007). However, without a full SED it is hard to distinguish between different categories (Padgett et al. 2006, Cieza et al. 2007), thus potentially distorting our understanding of this early evolutionary period.

3.2. Protoplanetary Disk Remnants

The mass of dust seen in debris disks is lower than that of protoplanetary disks, as illustrated in **Figure 3**, which shows dust masses derived from submillimeter observations of debris disks and protoplanetary disks. Although some protoplanetary disks are now seen down to 1 $M_\oplus$ (Andrews & Williams 2005), there is a distinction between >1 $M_\oplus$ protoplanetary disks and <1 $M_\oplus$ debris disks. Given that the mass of dust in debris disks is a small fraction of that of protoplanetary disks, it has been suggested that the protoplanetary disk clearing process is not 100% efficient and leaves behind a remnant population of solid material that is seen as a debris disk. In fact, this is the basis
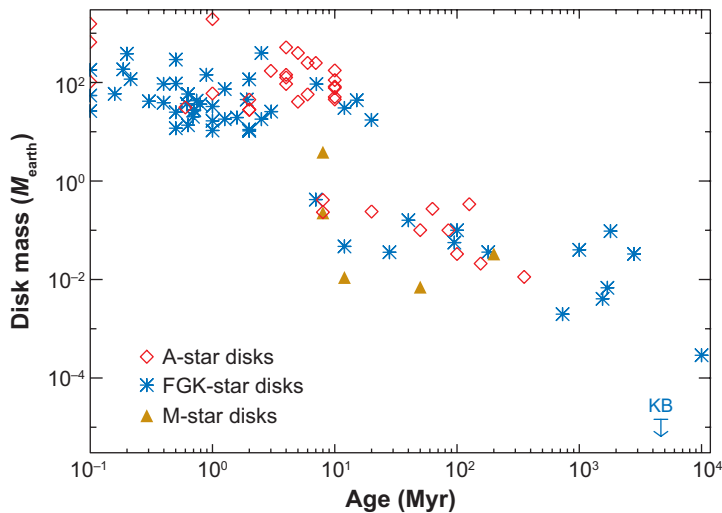

Figure 3

Evolution of disk mass derived from submillimeter observations. This plot extends the compilation of ages and masses of Wyatt, Dent & Greaves (2003) to include all debris disks currently detected at submillimeter wavelengths (Greaves et al. 2004b; Liu et al. 2004; Sheret, Dent & Wyatt 2004; Najita & Williams 2005; Wyatt et al. 2005; Lestrade et al. 2006; Williams & Andrews 2006; Matthews, Kalas & Wyatt 2007). The same (representative) sample of protoplanetary disks is included from Wyatt, Dent & Greaves (2003), and an opacity of 45 AU^2 $M_\oplus^{-1}$ is assumed for both protoplanetary and debris disks. The upper limit on the Kuiper belt dust mass from submillimeter observations (see Greaves et al. 2004b) is also plotted.

of all debris disk models. It may be more pertinent to ask what the size of the largest remnants is, and whether the remnant material is part of the less-than-centimeter-sized dust population seen previously in protoplanetary disk observations, or a population of greater-than-kilometer-sized planetesimals that subsequently produces dust through mutual collisions. The requirement for replenishment over >100-Myr timescales for the older debris disks argues for the latter scenario (Wyatt & Dent 2002). However, dust seen immediately following the transition need not be replenished over such long timescales, and some of the youngest (~10-Myr-old) debris disks may be remnant protoplanetary dust.

One problem with using a theoretical approach to answer whether young debris disks are protoplanetary dust remnants is that it is not yet known how protoplanetary dust is replenished. The growth of dust in protoplanetary disks from submicrometer- to meter-size is expected to occur rapidly through mutual collisions as the dust settles to the midplane through interaction with the gas (Dominik et al. 2007), yet the constant dust level observed throughout the 10-Myr protoplanetary disk lifetime (Natta et al. 2007) implies that grain growth cannot proceed indefinitely and there must be a mechanism replenishing the observed dust (Dullemond & Dominik 2005). Neither is it understood yet how (and when) planetesimals form in protoplanetary disks, because growth beyond the size of a meter is impeded by gas drag, which causes meter-sized objects to migrate into the star on timescales of 100 years. It is thought that perhaps rapid growth to sizes greater than a kilometer is facilitated by gravitational instabilities in a thin dust layer (Youdin & Shu 2002, Throop & Bally 2005), or through gas-dust interactions, which form local concentrations of boulders that undergo gravitational collapse (Johansen et al. 2007).

These uncertainties, along with those about the disk dispersal mechanism, preclude any definitive prediction for the dust and planetesimal populations that remain after the transition. However, this has been attempted within the context of the UV switch model by considering the evolution of a dust population embedded in the gas disk as it is being cleared (Alexander & Armitage 2007, Garaud 2007). In this model, less-than-millimeter-sized dust ends up concentrated in a ring close to the inner edge of the gas disk and gets swept out as that disk expands during the clearing phase. Several ways have also been identified in which gas-dust interactions might create rings of dust like those seen in debris disks, either by gas drag and photophoretic forces that concentrate small (micrometer-sized) dust in a ring at the outer edge of the gas disk (Takeuchi & Artymowicz 2001; Herrmann & Krivov 2007), or through an instability in a broad gas and dust distribution whereby a local dust enhancement heats the gas so that drag forces pull more distant grains into the ring, further promoting heating and grain concentration (Klahr & Lin 2001, 2005; Besla & Wu 2007). For these models to be relevant for determining the observable properties of a debris disk, and to affect our perception of its evolution, gas must be present in the debris disk phase, albeit in much lower quantities than in protoplanetary disks. These issues are explored further in Section 5.1.

3.3. Dust from Planet Formation Processes

Once kilometer-sized planetesimals have formed, the growth to larger objects like planets follows a better-defined path (e.g., Lissauer 1993; Goldreich, Lithwick & Sari 2004a; Papaloizou & Terquem 2006). A period of runaway growth, wherein the largest objects in the disk grow much faster than the remaining planetesimal population owing to gravitational focusing (Wetherill & Stewart 1989), is followed by a period of slower oligarchic growth, which occurs once the cores have grown to sufficient mass to dominate the velocity dispersion of nearby planetesimals (Kokubo & Ida 1998). After the planetary cores reach ~2000–3000 km in size, there follows a period of chaotic growth during which the orbits of protoplanets cross and scatter (Chambers & Wetherill 1998, Kenyon & Bromley 2006), resulting eventually in either collisional mergers or the ejection of one component,

with the latter occurring more often at large distances from the star (Goldreich, Lithwick & Sari 2004b).

The models of Kenyon & Bromley (2004a,b, 2005, 2006) make specific predictions for the amount of dust produced in this process. The quiescent level of dust during the initial runaway growth period is found to be relatively low. However, once the largest protoplanets have grown to 2000 km, their dynamical perturbations stir the population of <100-km planetesimals so that collisions among their population no longer result in net accretion, but have sufficient energy to be destructive. A collisional cascade is then initiated that depletes the <100-km population through the generation of dust, which is removed by radiation forces (see Section 4.1). In these models the timescale for the formation of 2000-km planetesimals depends only on the distance from the star and the surface density of solid material

$$t_{2000 \text{ km}} \approx 600(\Sigma_0/\Sigma_{\text{MMSN}})^{-1} r^3, \tag{12}$$

in years, where r is in AU, Σ_{MMSN} is the surface density in the minimum mass solar nebula (MMSN), and a surface density that falls off $\propto r^{-1.5}$ has been assumed (Kenyon & Bromley 2004a). Because planetesimal stirring takes longer further from the star, this is referred to as delayed stirring. An extended planetesimal disk in this model exhibits a ring of bright emission that moves to larger radius with time (Kenyon & Bromley 2004a). **Figure 4** shows the predictions of these models for the 24-μm emission from dust produced during planet formation in the terrestrial zone of a sun-like star (Kenyon & Bromley 2004b) and in a Kuiper belt around a 3-$M_\odot$ star (Kenyon & Bromley 2005).
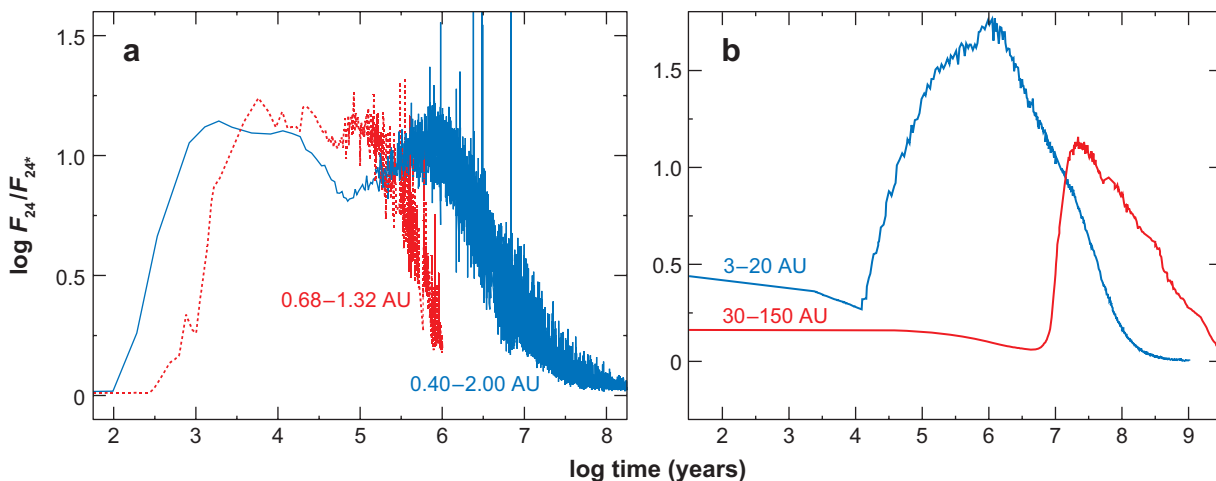

Figure 4

Predictions of planet-formation models for the detectability of dust produced in this process using 24-μm observations (Kenyon & Bromley 2005). The *y* axis shows the ratio of total flux to that of the star, and the *x* axis is the time since the model is started at which point kilometer-sized planetesimals are assumed to have formed already. Observations that can detect an excess ratio of 0.1 at 24 μm (e.g., Equation 10) imply a detectability limit of $\log F_{24}/F_{24*} > 0.04$ on these plots. In these models the level of dust emission remains low until the largest protoplanets reach 2000 km in size, at which point they stir the disk, resulting in a collisional cascade fed by 100-km planetesimals. (*a*) Model of terrestrial planet formation in the zones 0.68–1.32 AU (*red dashed line*) and 0.4–2 AU (*blue solid line*) around a sun-like star. Spikes in dust emission are seen when individual 100-km objects collide. (*b*) Model of planet formation in annuli at 3–20 AU and 30–150 AU from a 3-$M_\odot$ star. No spikes are seen from individual collisions at such large distances. Because the formation of 2000-km planetesimals takes longer further from the star, ~1 Gyr in this simulation at 150 AU, this is referred to as the delayed stirring, or self-stirring, model. Figure reproduced by permission of the AAS.

The amount of dust expected during this process remains debatable, because it depends on the uncertain prescriptions used to define the outcome of collisions at the different stages of planetesimal disk evolution. The clean-up of small bodies in the postoligarchy phase, and whether this affects the dynamics of the planet-formation process, is also not a solved problem (Goldreich, Lithwick & Sari 2004b; Leinhardt & Richardson 2005). Nevertheless the Kenyon & Bromley models indicate that dust produced in the context of the planet-formation paradigm can be detectable as a debris disk, a point underlined by the fact that in these models planet formation continues into the >10-Myr regime when the dust emission could only be classified as a debris disk.

Copious quantities of dust would also be expected in the aftermath of mergers between Mars-sized protoplanets, but the resulting level of dust emission and its subsequent evolution have yet to be quantified in the planet-formation models. Such events are expected to be common in the chaotic evolution phase, and may have resulted in the formation of the Earth-Moon and Pluto-Charon systems (Canup 2004, 2005), and may have determined the internal structure of Mercury (Asphaug, Agnor & Williams 2006). It has been suggested that the clump in the mid-IR structure of the 12-Myr β Pic disk (Telesco et al. 2005) and the planet imaged around 8-Myr 2M1207 (Mamajek & Meyer 2007), both of which are $\sim$50 AU from their stars, may be the hot remnants of such collisions.

Because the formation of gas giant planets necessarily occurs during the protoplanetary disk phase, that process cannot produce dust that can be detected as a debris disk. However, this process, and the consequences of having a planet in the disk, may have a direct influence on what is later seen as a debris disk, as well as on how that disk evolves (e.g., Section 4.3). It suffices to say that planets growing through collisions could grow to sufficient size to accrete gas from the surrounding disk, should any be left at this stage (Hubickyj, Bodenheimer & Lissauer 2005), although gas giant planets may also form rapidly through gravitational instabilities (Durisen et al. 2007). Planets may also end up far from the site where they formed through dynamical interaction with the gas disk (Papaloizou et al. 2007), a process that can significantly affect the distribution of planetesimals in the remnant debris disk (e.g., Lufkin, Richardson & Mundy 2006).

3.4. Summary

At the end of the protoplanetary disk phase, the star is expected to be surrounded by one or all of the following:

- planetary system, with planets ranging in size from those smaller than the Earth to those larger than Jupiter, the architecture of which may, or may not, be stable at this stage;
- remnant of the protoplanetary disk, both dust and gas;
- planetesimal belt in which planets continue to grow;
- planetesimal belt, which is being ground down to dust.

Different combinations of these categories could be present at different radial distances, and some radial locations could be empty. There is a wide range of protoplanetary disk masses, radii, and lifetimes from which to derive a wide range of possible outcomes. Additional diversity in outcome may result from differences in star-forming environment.

4. DEBRIS DISK EVOLUTION MODELS

This section considers the evolution of a planetesimal belt and the dust derived from it. Like the dust discussed in Section 2, the planetesimal belt is assumed to be in a uniform torus described by the parameters r, dr, and I. For much of this discussion, it is not necessary to consider the origin of the planetesimals that presumably formed within the protoplanetary disk. Their location could,

like the Solar System, be in the gaps in the planetary system where planetesimal orbits are stable on gigayear timescales (Lecar et al. 2001). However, such a configuration is not a prerequisite, and much of the discussion presented here is also applicable to other outcomes of protoplanetary disk evolution (Section 3).

4.1. Steady-State Collisional Evolution

If the planetesimal belt has been stirred so that collisions are destructive, i.e., if orbital eccentricities are greater than 10^{-3} to 10^{-2}, a collisional cascade will be set up in which planetesimals collide and are broken up into smaller objects that collide and are broken up into even smaller objects. In this way mass is passed to ever smaller dust sizes. For heuristic purposes, this section describes an idealized model of this process that was originally presented in Wyatt et al. (2007a), which is itself an extension of the earlier work of Dominik & Decin (2003).

The size distribution resulting from the steady-state evolution of an infinite collisional cascade follows a power-law with a well-defined slope

$$n(D) \propto D^{2-3q}, \tag{13}$$

where $q = 11/6$ (Tanaka, Inaba & Nagazawa 1996). It is estimated that the planetesimals feeding the cascade are of size $D_c = 1 - 100$ km (Wyatt & Dent 2002; Greaves et al. 2004b; Quillen, Morbidelli & Moore 2007). At the small-size end, particles below the size

$$D_{bl} = 0.8(L_\star/M_\star)(2700/\rho) \tag{14}$$

in μm, where ρ is density in kg m^{-3} (and is henceforth assumed to be 2700 kg m^{-3}), are removed by radiation pressure on dynamical timescales that causes an abrupt cut-off in the size distribution (Wyatt 2008). In the following, a distribution with $q = 11/6$ is assumed to extend from D_c down to D_{bl}, which means that most of the mass of the cascade is in the largest planetesimals, whereas most of its cross-sectional area is in the smallest dust, and that the fractional luminosity of the cascade is directly related its mass by

$$f/M_{tot} = 0.37r^{-2}D_{bl}^{-0.5}D_c^{-0.5}, \tag{15}$$

where r is in AU, D_c is in km, D_{bl} in μm, and M_{tot} is the total mass in objects of all size in $M_\oplus$. Equation 15 differs from Equation 7 in that M_{disk} corresponds to the mass of dust seen in the observation, whereas M_{tot} refers to the total mass of the cascade, the majority of which contributes little to the total observed flux.

Mass is lost from the cascade through the removal of the largest planetesimals, which occurs through mutual collisions on a timescale of

$$t_c = 1.4 \times 10^{-9}r^{13/3}(dr/r)D_cQ_D^{\star 5/6}e^{-5/3}M_\star^{-4/3}M_{tot}^{-1} \tag{16}$$

in Myr, where $Q_D^\star$ is planetesimal strength in J kg^{-1}, and e is mean planetesimal eccentricity, which is assumed to be equal to the inclination I of their orbits. Total disk mass evolves in the following way:

$$M_{tot}(t) = M_{tot}(0)/[1 + (t - t_{stir})/t_c], \tag{17}$$

where t_{stir} is the time at which collisions in the planetesimal belt become destructive; i.e., disk mass is constant at early times then falls off $\propto t^{-1}$. The fractional luminosity follows a similar evolution through Equation 15.

One consequence of this prescription for disk mass evolution is that the fractional luminosity (and mass) at late times is independent of the initial disk mass (Wyatt et al. 2007a), because disks

that start off with more mass simply process that mass faster to end up at the same level. Assuming that the collisional cascade is ignited early on, so that $t_{stir} \approx 0$, the maximum fractional luminosity a planetesimal belt of age t_{age} (in Myr) can have is

$$f_{max} = 0.58 \times 10^{-9} r^{7/3}(dr/r)D_c^{0.5} Q_D^{\star 5/6} e^{-5/3} M_\star^{-5/6} L_\star^{-0.5} t_{age}^{-1}. \tag{18}$$

I refer to the assumption that $t_{stir} = 0$ as a prestirred planetesimal belt.

Although there is considerable flexibility in the values of D_c, $Q_D^\star$, and e that a planetesimal belt could have, it was found that the population of debris disks around A stars could be fitted by assuming all have an evolution described by Equations 17 and 16 with $e = 0.05$, $D_c = 60$ km, and $Q_D^\star = 150$ J kg^{-1}, also assuming $dr/r = 0.5$ and taking r from the 24/70-μm flux ratio and Equation 3 (Wyatt et al. 2007b; see Section 5.1.1). Thus, these parameters can be used as a first estimate of a debris disk's evolution, assuming it is in steady state. **Figure 5** shows evolutionary tracks using these assumptions for planetesimal belts of radii 10, 30, and 100 AU and initial masses of 0.1, 1, and 10 $M_\oplus$. Putting the same mass closer to the star results in a higher initial disk luminosity, but also results in faster processing times.

The above model neglects some details. First, planetesimal strength varies with size, which modifies the equilibrium slope of the size distribution from $q = 11/6$ (O'Brien & Greenberg 2003), sets up a wave in the size distribution (Durda, Greenberg & Jedicke 1998), and means that the pre-equilibrium evolution may not be exactly flat. Second, it makes idealistic assumptions about the size distribution at the small-size end, which is wavy because of the abrupt cut-off below D_{bl} (Thébault, Augereau & Beust 2003), and which also extends to larger radii because of the effect of radiation pressure on dust close to and below the blow-out limit (Wyatt et al. 1999). All of these issues have been explored in more depth using numerical modeling to evolve the size and spatial distribution of material in a planetesimal belt (Krivov, Löhne & Sremčević 2006; Thébault & Augereau 2007). Such models are indispensable when interpreting a disk's detailed structure; e.g., such models show that the dust of β Pic and AU Mic, seen in scattered light out to thousands of astronomical units, actually derives from planetesimal belts at 40–100 AU (Augereau et al. 2001, Strubbe & Chiang 2006). They also demonstrate that the evolution in dust luminosity is flatter ($\propto t_{age}^{-0.3}$) than that given in Equation 17, and that dust mass and total disk mass evolve differently because the size distribution also evolves with time. This means that dust luminosity at late times can include a dependence on initial mass (Löhne, Krivov & Rodmann 2008). Nevertheless, the prescription given by Equations 15–18 provides an estimate of fractional luminosity that agrees with that of the more detailed numerical model to within an order of magnitude for reasonable disk parameters.

Poynting-Robertson (P-R) drag has thus far been ignored. This makes small dust spiral into the star on timescales of $t_{pr} = 400\beta^{-1}r^2 M_\star^{-1}$ years, where β is the ratio of the radiation force to that of stellar gravity, which is particle-size dependent (but not distance-from-the-star dependent) and is ≤ 0.5 for bound grains. Thus, P-R drag provides an alternative mechanism for removing small grains from the cascade. Dust in the Solar System is significantly influenced by P-R drag, because dust <1 mm created in the asteroid belt is seen to spiral into the Sun past the Earth (Dermott et al. 2001), and the dust created in the Kuiper belt extends interior to Neptune (Liou & Zook 1999, Moro-Martín & Malhotra 2002). For the known debris disks, P-R drag can be ignored (Wyatt 2005a), as the collisional lifetime of the smallest dust, $t_{coll} = 0.04 r^{1.5} M_\star^{-0.5}(dr/r)f^{-1}$, is shorter than its P-R drag lifetime, unless the disk is below the limit of detectability (see Section 5.1.1). The low fractional luminosity of the Solar System's debris disk means it operates in a regime where P-R drag is important. However, stellar winds provide a force acting on dust grains that is analogous to P-R drag, and which can be 10–1000 times stronger than P-R drag for young and late-type stars, which would mean it can no longer be ignored (Plavchan, Jura & Lipsky 2005).
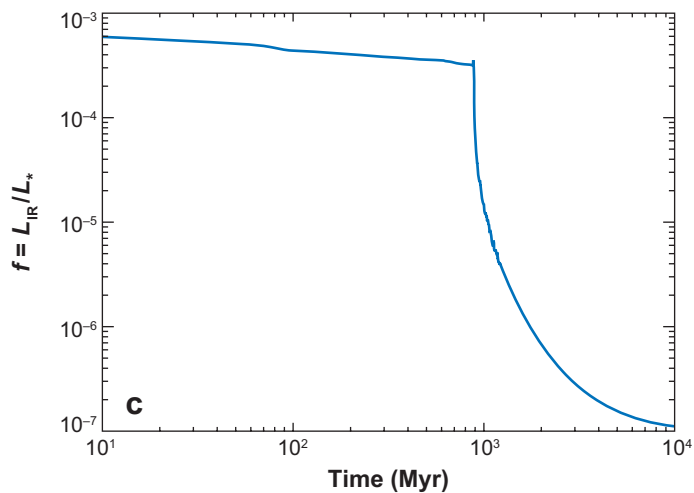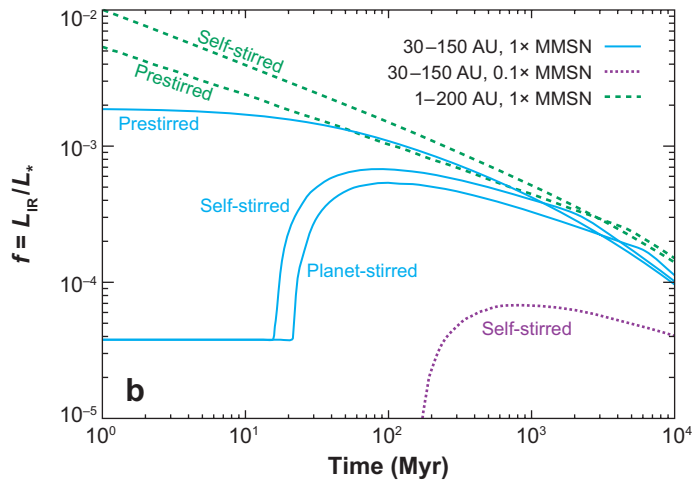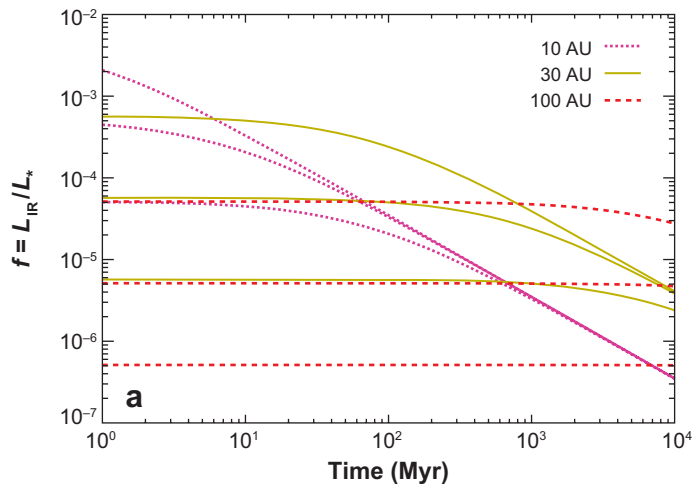
The evolution of planetesimal belts in which P-R or stellar wind drag are the dominant mechanisms for removing small grains is such that, while their mass still falls off $\propto t^{-1}$ (Equation 17), their fractional luminosity is reduced below that predicted by Equation 15 and falls off $\propto t^{-2}$ (Dominik & Decin 2003).

4.2. Stochastic Collisions

Although collisions between the largest planetesimals in a planetesimal belt occur infrequently, they can release large quantities of small dust that then decays through its subsequent collisional and dynamical evolution. Thus individual collisions can introduce a stochastic component to a debris disk's population of small dust. Dust bands in the structure of the zodiacal cloud (Low et al. 1984) have been identified with collisions between 10- to 100-km asteroids in the asteroid belt (Nesvorný et al. 2003), and are testament to the stochastic evolution of the Solar System's debris disk. They also show that dust produced in such events can persist over 10-Myr timescales, further evidence for which lies in deep sea sediments of dust accreted by the Earth (Farley et al. 2006).

However, single collisions cannot typically be responsible for observed debris disk emission, because the dust mass needed to make a debris disk detectable implies that such massive events are rare; e.g., Wyatt & Dent (2002) concluded that >1400-km planetesimals are required to be completely pulverized to make a detectable signature in the Fomalhaut disk, and that such a signature might be detectable for just 1–2% of the disk's lifetime. A similar conclusion was reached by Kenyon & Bromley (2005), who found that while collisions close to the star at <3 AU are detectable, there is no detectable increase in emission spectrum following planetesimal collisions at >3 AU (see **Figure 4**). This is understandable when considering the fractional luminosity resulting from turning a planetesimal of size D_c into D_{bl}-sized dust:

$$f_{coll} = 2.8 \times 10^{-9} D_c^3 D_{bl}^{-1} r^{-2}. \qquad (19)$$

Collisions in the Solar System are detectable because the quiescent dust level is so low; turning a 10-km asteroid into 1-μm dust at 3 AU results in $f_{coll} = 3 \times 10^{-7}$, which is larger than the current level of 0.8×10^{-7} (Backman & Paresce 1993). However, our chances of witnessing collisions between massive protoplanets may be relatively high in young systems in which planet formation processes are ongoing (see Section 3.3).

Although dust created in a single collision may be unlikely to be detectable, it is also possible that it is the ignition of the collisional cascade that is stochastic. Collisions are one possible trigger explored in the collisional avalanche model of Grigorieva, Artymowicz & Thébault (2007) in which small collisionally produced dust collides with grains in the quiescent disk, further enhancing the small dust population. This mechanism operates on dust that is small enough to be strongly

---

Figure 5

Models for the evolution of planetesimal belts and the fractional luminosity of dust derived from them. (*a*) Steady-state collisional evolution model in which the dust level is constant until the largest planetesimals reach collisional equilibrium, whereupon the level falls off $\propto t^{-1}$ (Wyatt et al. 2007b; Section 4.1). The evolution of 10-, 30-, and 100-AU belts are shown for starting masses of 0.1, 1, and 10 $M_\oplus$, from bottom to top, respectively. (*b*) Delayed stirring models wherein a planetesimal belt extending from 1–200 AU or 30–150 AU evolves assuming it is prestirred ($t_{stir} = 0$ at all radii), self-stirred ($t_{stir} = t_{2000\,km}$, i.e., stirred when 2000-km objects form), or stirred by the secular perturbations of a Jupiter-mass planet at 3 AU (Section 4.3). MMSN refers to a mass surface density equivalent to a minimum mass solar nebula (Equation 20). (*c*) Late heavy bombardment model in which the Kuiper belt is depleted at 880 Myr by a dynamical instability when Jupiter and Saturn cross the 2:1 resonance (Gomes et al. 2005; Section 4.4).

affected by radiation pressure (because such dust grains have high relative velocities with respect to quiescent disk material) and can set off a runaway reaction. However, to do so requires a large optical depth in the plane of the disk, and so may only be applicable to debris disks denser than β Pic.

4.3. Delayed Stirring

The majority of the discussion of the steady-state evolution model in Section 4.1 assumed that the collisional cascade was started at $t = t_{stir} = 0$. However, the ignition of the collisional cascade requires some mechanism to stir the disks. The planet-formation models of Kenyon & Bromley (2004a) treat the stirring self-consistently in that the disk is stirred by the gravitational perturbations of material within the planetesimal belt, and a collisional cascade is initiated once planetesimals have grown to 2000 km (see **Figure 4** and Section 3.3). I will refer to this as self-stirring.

Here the analytical equations of steady-state collisional evolution are used to consider the implications of the self-stirring models. To do so it is assumed that there is an extended planetesimal belt and that at each radius the cascade is initiated later on according to Equation 12, so that $t_{stir} = t_{2000\,km}$. Before the cascade has been initiated (i.e., at $t < t_{2000\,km}$), the ratio of fractional luminosity to mass is some fraction, say 2%, of that given by Equation 15. Under these assumptions **Figure 5** shows the evolution of planetesimal belts undergoing self-stirring, both for a broad belt (1–200 AU) and for a belt with a restricted range of radii (30–150 AU). The mass surface density in the belts is scaled to a $1 \times$ minimum mass solar nebula (MMSN) in which

$$dM/dr = 10 M_\oplus r^{-0.5}. \tag{20}$$

Comparison with figure 7 of Kenyon & Bromley (2005) shows good qualitative agreement, implying that the detailed physics of the planet-formation models, at least in terms of the amount of detectable dust produced, can be reproduced by a simple analytical formulation.

The evolution of planetesimal belts undergoing self-stirring is also shown for comparison with equivalent belts that are prestirred, i.e., in which $t_{stir} = 0$ at all radii. For the belt that extends 1–200 AU, there is little difference between the two models. However, for planetesimal belts that have inner cleared regions 30 AU in radius, the effect of the delay in the onset of stirring is to cause a low disk luminosity until the collisional cascade is ignited at the inner edge of the belt. The time at which that happens is set by both the radius of the inner cleared region and the surface density (Equation 12), as illustrated by comparison of the evolution for belts 30–150 AU wide and of $0.1 \times$ and $1 \times$ MMSN densities. The jump that occurs when the cascade is ignited depends on the change in size distribution from the planetesimal accumulation phase ($t < t_{2000\,km}$) to that in the collisional cascade phase ($t > t_{2000\,km}$). Here the dust content in the accumulation phase was reduced by $\sim$50 compared with Equation 15. Although this is comparable with the evolution seen by Kenyon & Bromley, it is important to remember that the amount of dust present during the epoch of ongoing planet formation is not well understood (Section 3.3).

The origin of the stirring in the prestirred models is not specified. The formation of a 2000-km object is not necessarily required to stir the belt. For example, Moro-Martín et al. (2007) consider how the two known planets in the HD 38529 system interact with planetesimals in their debris disk, and point out that the planets' secular perturbations would excite eccentricities that promote collisions, thus depleting the disk. **Figure 5b** also shows the fractional luminosity evolution of a 30- to 150-AU planetesimal belt under the same assumptions as for the self-stirred model described above, except that the delay in onset of the collisional cascade is set not by the formation of 2000-km planetesimals, but by the secular precession timescale of a Jupiter-mass planet on an eccentric orbit at 3 AU from a 1-$M_\odot$ star. The planet's secular perturbations stir material closer to its orbit faster

than that further away (Wyatt 2005b), and for this planet configuration the secular perturbation timescales are similar to the timescale for growth to 2000-km size at most distances. Although this is a simplification of the dynamics of this interaction (see, e.g., Thébault, Marzari & Scholl 2006), it shows that giant planets formed close to the star can perturb the disk out to large distances, even before 2000-km objects have formed. Perturbations from binary companions could stir the belt in a similar manner, and smaller, say Neptune-mass, planets orbiting close to the inner edge of the belt would also stir the disk through both secular and resonant perturbations; e.g., the secular perturbations of a Neptune-mass planet at 15 AU take 10 Myr to be felt at 30 AU.

One obvious prediction of the delayed stirring models (either the self-stirred or planet-stirred models) is an increase in disk radius with age. The steady-state evolution of a prestirred extended planetesimal belt would also exhibit a radius that increases with time; the inner regions clear out rapidly, resulting in a surface density $\propto r^{7/3}$ (Equation 18), whereas the surface density falls off in the outer regions in accordance with the initial surface density distribution, resulting in a broad ring in which the peak in surface density moves to a larger radius with age. A belt undergoing self-stirring has a similar surface density profile, except that it has a sharper inner edge (because of the delay in stirring) and a sharper outer edge (because the outer regions are still undergoing accretion). A belt that is truncated by a planet also has an inner edge with a slope that is dependent on planet mass (Quillen 2006). Thus the radial profile of imaged debris disks can provide valuable information on the nature of the planetary system and the possibility that planet formation is ongoing within them.

4.4. Planetary System Shake-Down

Planetary system architecture is not necessarily set in the protoplanetary disk phase. There may be significant evolution as the planetary system settles into a stable configuration. This can have a profound effect on the debris disk. Likewise the debris disk can have a profound effect on the shake-down process.

Although the Solar System planet orbits are stable for 4.5 Gyr, the evolution of the terrestrial planets, asteroids and Kuiper belt objects may be chaotic on longer and shorter timescales (Lecar et al. 2001); it must be remembered that what remains in the Solar System today is just the stable remnant of the initial constituents of the planetary system and debris disk. Evidence for significant restructuring during the Solar System's evolution is present in the dynamical structure of its debris disk and in the cratering records of the terrestrial planets and the Solar System's moons. For example, the dynamical structure of the Kuiper belt provides evidence for sculpting by the migration of Neptune (Chiang et al. 2007; Morbidelli, Levison & Gomes 2008), and age dating of lunar samples shows that the cratering rate on the Moon was much higher in the first 600–800 Myr than its subsequent rate (see review in Hartmann et al. 2000), with present evidence favoring a terminal cataclysm that occurred 3.8–4.0 Gyr ago rather than a slow decline in impact cratering from the time of formation (Bottke et al. 2007). The cataclysmic event that occurred ~700 Myr after the Solar System formed is referred to as the Late Heavy Bombardment (LHB), and is thought to have been characterized by a high flux of planetesimals that originated in the asteroid belt, but which then spread throughout the inner Solar System (Strom et al. 2005).

To explain these various observations it has been suggested that Uranus and Neptune formed between Jupiter and Saturn (Thommes, Duncan & Levison 1999), that the Solar System formed in its current configuration but with the outer planets on tighter orbits (Tsiganis et al. 2005, Thommes et al. 2007), or that the Solar System formed with many planets like Uranus and Neptune, some of which have since been lost (Chiang et al. 2007; Ford & Chiang 2007). In all of these models, the planetary system is either inherently unstable or is pushed to instability through interaction

with the remnant planetesimal disk. The planetesimal disk exchanges angular momentum with the planets causing the relative spacing of their orbits to change (Fernández & Ip 1984), which can lead to planet pairs crossing resonances, thus causing increases in eccentricity and potentially leading to dynamical instability. This instability can result in the scattering or ejection of one or more of the ice giant planets, which through further interaction with the planetesimal disk can have their orbits circularized and migrated outward (Hahn & Malhotra 1999; Gomes, Morbidelli & Levison 2004; Levison et al. 2007). Although these models can explain many of the dynamical constraints of the Solar System, including the LHB (e.g., Tsiganis et al. 2005, Gomes et al. 2005, Morbidelli et al. 2005), they rely on assumptions about the rather uncertain outcome of the planet-formation process. However, they also indicate that instability may be a common occurrence for planetary systems that end up with Solar System-like configurations, and that this can occur after up to 1 Gyr of quasi-stable evolution (Gomes et al. 2005, Thommes et al. 2007).

The high eccentricities of the known extrasolar planets (Udry & Santos 2007) may also be evidence for chaotic dynamical evolution in planetary systems that are unlike our own. For example, Jurić & Tremaine (2007) find that randomly constructed multiple planetary systems would undergo a 100-Myr period of dynamical instability after formation in which planet-planet scattering would cause ejections, mergers, and eccentricity pumping, leading to a final eccentricity distribution that is similar to that observed (see also Ford & Rasio 2007). Although these models also rely on assumptions about the outcome of planet formation, they do point to the possibility that instabilities are a common occurrence for planetary systems that end up with exoplanet-like configurations.

A search for evolution in the eccentricity distribution with age in the <100-Myr period (e.g., Takeda et al. 2007) is one way to probe the early dynamical evolution of planetary systems. However, debris disks have the potential to provide similar information, because the different models for the settling period should make different predictions for the appearance of debris. Such predictions have yet to be made, because they are not the primary focus of planet formation studies, although it can be seen that a wide array of planetesimal belt masses and radii result from similar starting conditions (Thommes et al. 2007). **Figure 5** shows the evolution of fractional luminosity of Kuiper belt material in the model for Solar System evolution of Gomes et al. (2005) (M. Booth, manuscript in preparation; see also figure 5 of Meyer et al. 2007) and uses Equation 15 to convert between mass and fractional luminosity in those models. It is clear that planet-formation models can readily make predictions for the detectability of debris that can be compared critically against debris disk statistics (see Section 5.2).

4.5. Cometary Sublimation

Although this section has focused on a dust component derived from collisions in a planetesimal belt, it is evident that dust released in comet sublimation also permeates the inner Solar System (Sykes et al. 1986), even if the relative contribution to the zodiacal cloud from asteroids and comets remains uncertain (Kortenkamp & Dermott 1998, Ipatov et al. 2008). Cometary sublimation may enhance (or even dominate) the dust population in some debris disks (e.g., Jura et al. 1998). However, because comets sublimate at 110 K, and debris disks have a range of temperatures mostly below 110 K, this can only be relevant for the few hottest debris disks (or for the hottest dust components of debris disks). From an evolutionary perspective, it is worth noting that single objects can significantly affect the observability of a debris disk, because a 1000-km-sized supercomet trapped on a circular orbit 1 AU from a sun-like star could release sufficient dust over a long enough timescale for it to be detected (Beichman et al. 2005); a swarm of 10^6 Hale-Bopp-sized comets would be needed to produce an equivalent level of emission.

4.6. External Processes

All of the above models for disk evolution involve processes internal to the planetary system. External processes can also either directly affect debris disk evolution or affect our perception of it. For example, a close encounter with a nearby star, such as that which may have truncated the Kuiper belt (Levison, Morbidelli & Dones 2004), would significantly alter a debris disk's structure (Larwood & Kalas 2001) and could initiate a collisional cascade in the outer regions (Kenyon & Bromley 2002). However, the low space density of nearby stars means that close encounters occur infrequently, once every 10^{10} years for encounters of <500 AU, and so should affect only a minority of debris disks, although such encounters may have been more common in the protoplanetary disk phase (Adams & Laughlin 2001, Scally & Clarke 2001). Also, passage through a dense region of the interstellar medium (ISM) could both sandblast a debris disk—resulting in an enhanced population of small dust—or result in an enhanced infrared luminosity from interstellar dust heated by the star. Sandblasting may be insignificant due to radiation pressure that clears a cavity around the star (Artymowicz & Clampin 1997). However some stars that exhibit excess infrared emission are inferred to be heating, or otherwise interacting with, nearby interstellar dust. Although such stars are typically beyond $\sim$120 pc (Kalas et al. 2002, Kalas 2005, Stauffer et al. 2005), there have been more recent detections of this phenomenon within the low-density local bubble [HD61005 (Hines et al. 2007) and δ Vel (Gáspár et al. 2008)]. Its relatively large beam size means that excesses discovered with IRAS have also been found to originate in background stars (Lisse et al. 2002) and galaxies (Kalas et al. 2002; Sheret, Dent & Wyatt 2004). Such bogus disks can be weeded out in detailed studies (Moór et al. 2006; Rhee et al. 2007; Smith, Wyatt & Dent 2008), but are not thought to significantly affect survey statistics in which their incidence would be expected to have a flat age distribution.

5. CONSTRAINTS FROM OBSERVATIONS ON DEBRIS DISK EVOLUTION

Having laid down the general ideas on how debris disks either are expected to or could plausibly evolve, this section presents the observational results that constrain how debris disks actually evolve. **Figure 1c** shows how the statistics are expected to be strongly biased by spectral type. There may also be a more fundamental difference between the disks of stars of different spectral types, e.g., in their mass distribution (Greaves & Wyatt 2003) or in the physics affecting their dust evolution (Plavchan, Jura & Lipsky 2005). Thus the results for A stars, sun-like stars (FGK stars), and M stars are discussed here in separate sections. The section concludes with a discussion of the role of debris disk imaging in our understanding of disk evolution.

5.1. A Stars

The evolution of A-star debris disks at 24 and 70 μm has been well characterized by the surveys of Rieke et al. (2005) and Su et al. (2006), the statistics from which are shown in **Figure 6**. Rieke et al. (2005) performed a 24-μm survey of 266 main sequence A stars with ages in the range of 5–850 Myr, reaching a calibration-limited sensitivity of $R_{v\,\mathrm{lim}} = 0.1$. They found that younger stars exhibit excess emission more frequently and with higher fractional excess than older stars, and showed that the upper envelope of 24-μm fractional excess falls off inversely with age with a characteristic timescale of 150 Myr. From the large number of young stars without 24-μm excess, they concluded that half of stars emerge with little in the 10–60 AU region, and from the large spread in excess at all ages they suggested that bright excesses may arise from stochastic evolution
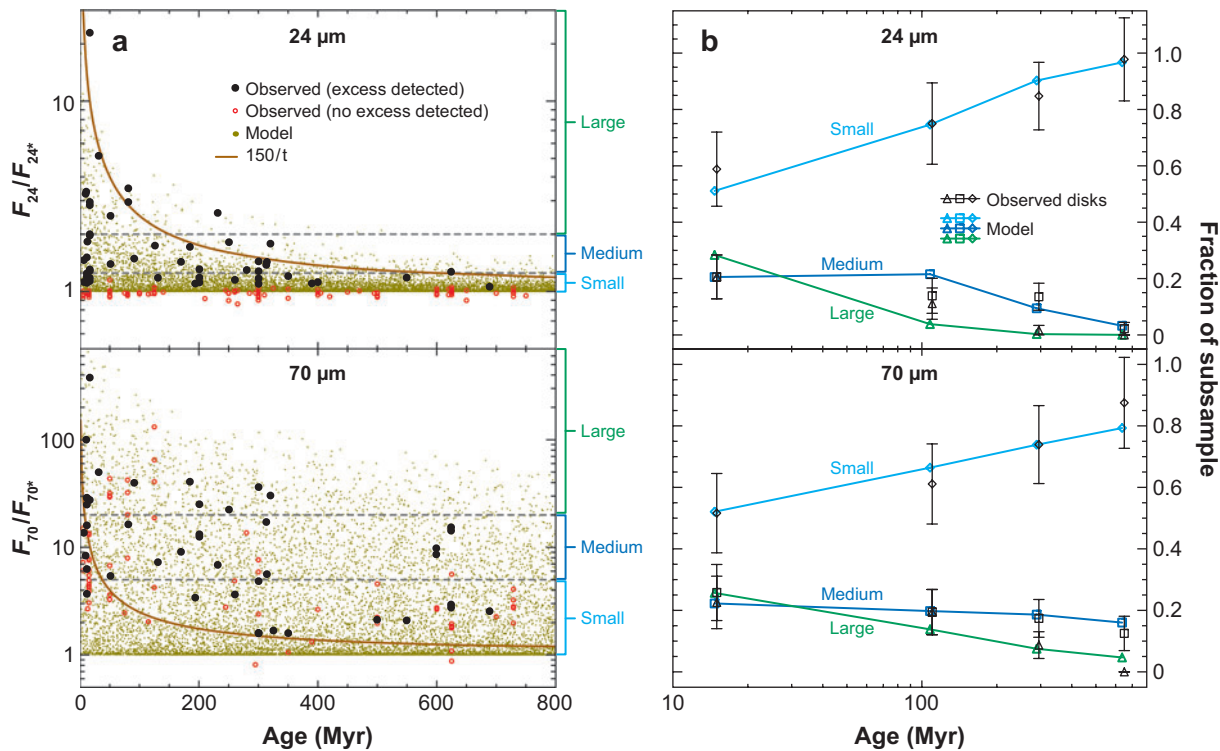
Figure 6

Evolution of the 24-μm (*top*) and 70-μm (*bottom*) fractional excesses of A stars (Rieke et al. 2005, Su et al. 2006, Wyatt et al. 2007b). (*a*) Fractional excess of observed disks (*black closed circles and red open circles*) and a model population (*yellow dots*), in which all A stars possess a prestirred planetesimal belt with a range of initial masses (a log-normal distribution centered on 10 $M_\oplus$ of width 1.14 dex) and radii (3–120 AU), and which all undergo steady-state evolution. (*b*) Fraction of stars with fractional excesses defined as small, medium, and large for four age bins. Observed statistics are shown with symbols and error bars. The statistics for the model population are shown with symbols and lines. The steady-state evolution model simultaneously reproduces both the 24- and 70-μm observed statistics. Thus there is no need to invoke anything beyond steady-state evolution for the majority of the A-star population to explain these observations, although detailed study of individual disks shows that there are exceptions where a stochastic component to the evolution is inferred, and the origin and timing of the stirring of the belts remain uncertain.

wherein disks brighten following recent collisions (Section 4.2). Su et al. (2006) performed an analogous 70-μm survey to a calibration limit of $R_{\nu\,\text{lim}} = 0.55$, although the observations of more distant stars were sensitivity limited. The 70-μm results are similar to those at 24 μm, except that the emission is seen to persist for longer and up to a higher fractional excess, implying that clearing is more rapid in the inner regions that are probed by the shorter wavelength observations. Over all ages it was found that about one-third of A stars exhibit excess at 24 and/or 70 μm, illustrating the ubiquity of the debris disk phenomenon.

5.1.1. Steady-state interpretation. The evolution of both the 24- and 70-μm emission from A stars can be explained simultaneously by a model that assumes that all A stars have a prestirred planetesimal belt, and that belt has a range of possible initial masses (a log-normal distribution centered on 10 $M_\oplus$ of width 1.14 dex, similar to protoplanetary disks) and a range of possible radii (3–120 AU); each planetesimal belt is assumed to evolve in steady-state according to the prescription given in Section 4.1 (Wyatt et al. 2007b; see **Figure 6**). A spread in excess is seen
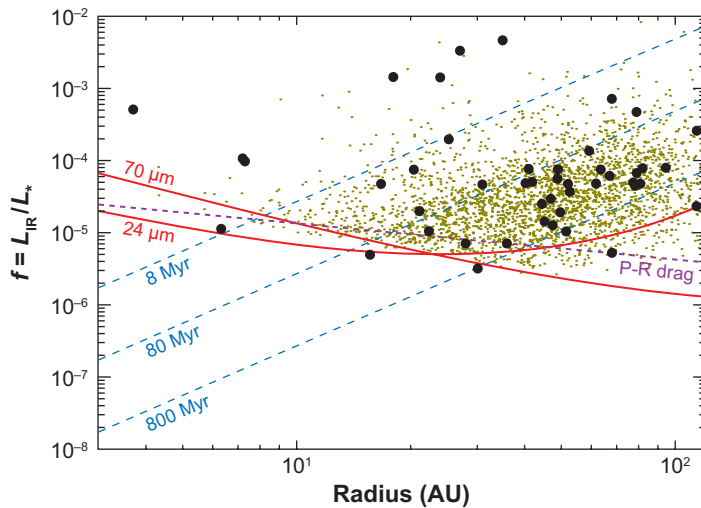
Figure 7

Fractional luminosity versus radius of A-star debris disks detected at 24 and 70 μm (Wyatt et al. 2007b). Disks detected with *Spitzer* or IRAS at both wavelengths are shown with black circles, whereas the subset of the model population undergoing steady-state evolution (see **Figure 6**) that could have been detected at both wavelengths is shown with yellow dots. The detection thresholds for A0V stars (Equation 11) at 24 and 70 μm are shown with solid red lines; disks must be above these lines to be detected at these wavelengths. The lines of maximum fractional luminosity for ages of 8, 80, and 800 Myr are shown with dashed lines (Equation 18); disks at these ages must lie on or below these lines. The disks that are above the 8-Myr line are either around 5- to 12-Myr-old stars or are, like ζ Lep, unusually bright for their age and so may be indicative of a recent brightening event. The dotted purple line shows the limit at which P-R drag becomes important (see Section 4.1); for disks below this line, P-R drag may need to be taken into account when considering their evolution.

at all ages in the model, both because of the distribution of initial masses and because of the distribution of belt radii. Thus the observed range in excesses cannot be taken as evidence for stochastic evolution. The distribution of radii was inferred from that of disks detected at both 24 and 70 μm, which peaks around 45 AU. The observed radius distribution is biased in a way best explained by referring to **Figure 7**, which shows fractional luminosity versus radius for A-star disks detected at 24 and 70 μm, along with the detection thresholds (Equation 11). Not only is disk detectability a function of belt radius (Section 2), but close-in belts also lose mass at a faster rate than those at larger distance (Equation 16), which is illustrated by the upper bound in fractional luminosity for disks with ages of 8, 80, and 800 Myr (Equation 18). By comparison with the model population that could be detected at 24 and 70 μm, it was inferred that the underlying radius distribution actually follows $N(r) \propto r^{-0.8}$ between 3–120 AU, where $N(r)\delta r$ is the number of planetesimal belts with radii between r and $r + \delta r$. Most of the biases in the observed statistics can be explained through reference to **Figure 7**, such as why disks detected at 24 but not 70 μm are younger than average (Su et al. 2006), and why the average radius of detectable disks in the model population increases with time even though individual disks have a fixed radius (Wyatt et al. 2007b).

5.1.2. Requirement for stochasticity. Although the steady-state evolution model explains a significant body of observational statistics, there are several important exceptions. For example, the archetypal debris disk Vega provides evidence in favor of stochastic evolution (Section 4.2).

Contrary to submillimeter observations that showed the dust to be within 200 AU (Holland et al. 1998), dust is seen out to 800 AU at 24 and 70 μm (Su et al. 2005; see **Figure 8**). Both the dust size that is inferred from its temperature and the measured dust spatial distribution are consistent with that expected from dust being expelled by radiation pressure. The inferred mass-loss rate of ∼2 $M_\oplus$ Myr^{-1} (Su et al. 2006, Wyatt 2006) could not have been sustained over the 350-Myr lifetime of Vega, posing a problem for steady-state models that anticipate a mass-loss rate of ∼M_{tot}/t_{age}, i.e.,

$$M_{tot}/t_{age} = 4.2 \times 10^9 f^2 r^{-1/3} (dr/r)^{-1} Q_D^{\star -5/6} e^{5/3} L_\star M_\star^{1/3}, \tag{21}$$

in $M_\oplus$ Myr^{-1}, which is ∼0.01 $M_\oplus$ Myr^{-1} for Vega (see also Krivov, Löhne & Sremcević 2006). It is suggested that the observed radiation pressure component is a transient component sitting on top of a planetesimal belt evolving in steady state (Su et al. 2005), possibly created in a recent collision or in a recent ignition of the collisional cascade in one part of the disk. It is not yet known how common systems with transient components like Vega are. Such stochasticity may present only minor perturbations to the underlying steady-state evolution of a debris disk's fundamental parameters. Further support for a stochastic component to A-star debris disk evolution comes from a clump at 52 AU in the β Pic disk, which has been attributed to a recent collision between massive protoplanets (Telesco et al. 2005; see **Figure 8**).

Close-in A-star disks also pose a problem for steady-state models. For example, ζ Lep hosts dust with a temperature of ∼320 K (Chen & Jura 2001) seen to lie at 2–8 AU (Moerchen et al. 2007b; see **Figure 8**). At such a distance the level of fractional excess is above the maximum possible at this age for steady-state processing (Equation 18; Wyatt et al. 2007b). In other words, the initial mass of the planetesimal belt cannot be increased to elicit a higher luminosity at this age (although see Löhne, Krivov & Rodmann 2008). However, before it can be concluded that the observed dust is transient, it must be noted that this system could simply have planetesimal belt properties that differ from the rest of the A-star disk population (Wyatt et al. 2007b), e.g., with unusually low eccentricities or high planetesimal strength and/or size. It might be expected that these properties depend on radius, because inner planetesimal belts may be composed of rock rather than ice. Nevertheless, near-IR interferometry provides evidence for hot dust even closer to some A stars (Absil et al. 2006; R. Akeson, private communication), where steady-state production in a planetesimal belt colocated with the dust is extremely unlikely.

5.1.3. Possible role for delayed stirring.
There is also evidence that supports the delayed stirring model (Section 4.3). Rhee et al. (2007) reanalyzed the IRAS database and found that the upper envelope in radius increases with age for A/B stars (their figure 7). No increase in radius for A-star planetesimal belts was seen by Wyatt et al. (2007b), which may be because the 13 cool (>120 AU) disks of Rhee et al. found at late ages were detected by IRAS at 60 and 100 μm, whereas the Wyatt et al. sample only included disks detected at 24 and 70 μm. These old cool disks, which have yet to be confirmed by *Spitzer* (Rhee et al. 2007), merit closer inspection. The delay in appearance of bright emission at >120 AU is consistent with the expected evolution of primordial disks with <10 × MMSN undergoing self-stirring (Equation 12), which could suggest that this observation is evidence that planet formation continues to hundreds of AU for some A stars even as old as a few hundred million years. However, an apparent increase in radius with time is also expected from prestirred steady-state evolution models (Section 4.3). Measurement of the radial profile of the inner edge of the belt may be able to distinguish between the different models. For one 200-Myr A star with a belt at 133 AU (Fomalhaut), the steep inner profile (Kalas et al. 2005) suggests that a planet rather than collisional grinding is truncating the inner edge (Quillen 2006).
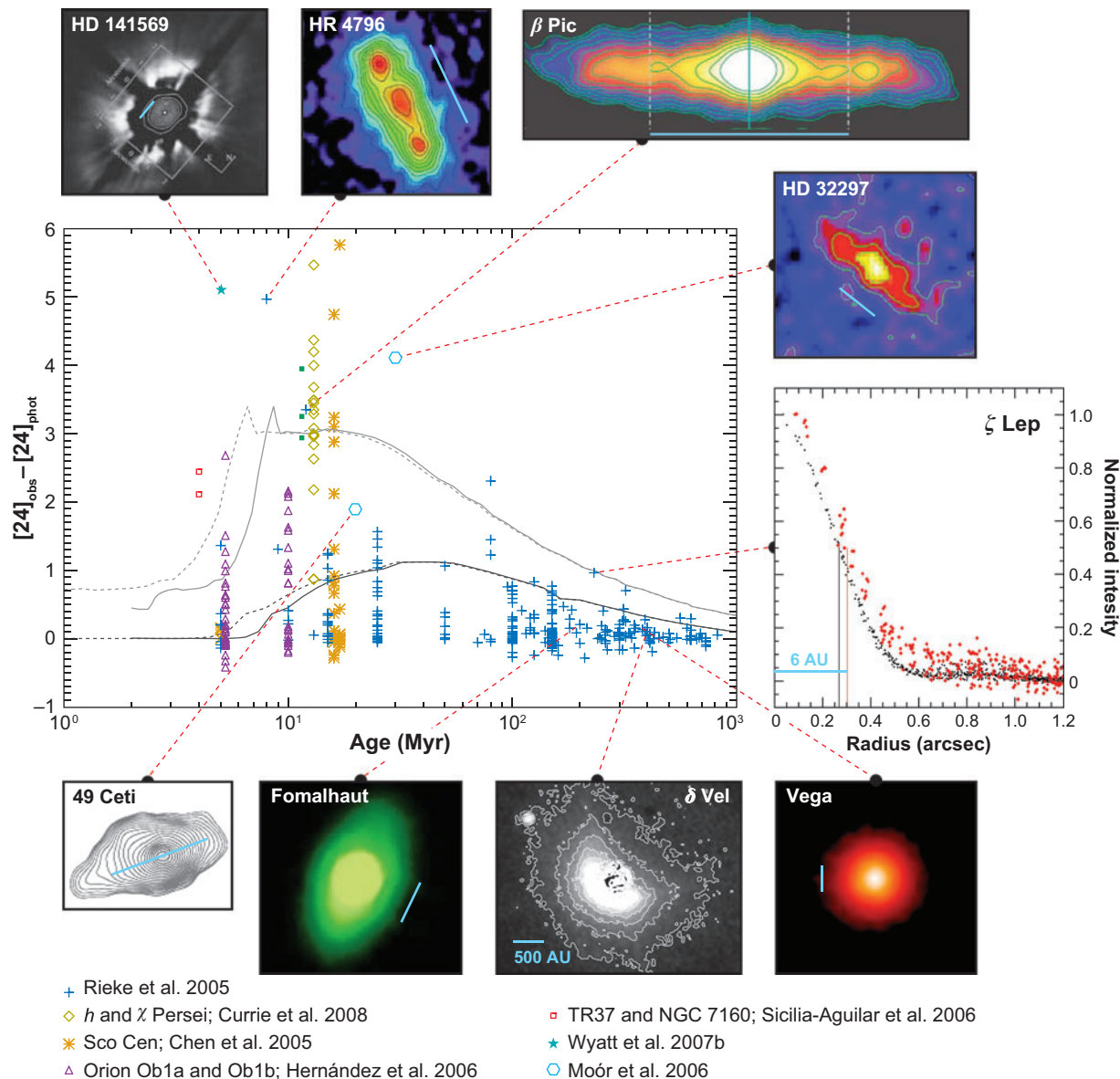
Figure 8

Fractional excess of A stars at 24 μm as a function of age (Currie et al. 2008). The fractional excess increases from 5 Myr to a peak at 10–15 Myr, followed by a decline with age. This plot includes A stars thought to have debris disks, but excludes the few optically thick protoplanetary disks from the <10-Myr samples, such as HD 290543 at 5 Myr with $[24]_{obs} - [24]_{phot} = 6.8$ (Hernández et al. 2006). The lines show the self-stirred models of Kenyon & Bromley (2005) for a planetesimal belt extending 30–150 AU that has a mass distribution $3\times$ and $1/3\times$ MMSN. Mid-IR (18–25 μm) images of specific disks are overplotted to illustrate where this emission comes from at different ages: HD 141569, Fisher et al. 2000; HR 4796, Telesco et al. 2000; β Pic, Telesco et al. 2005; 49 Ceti, Wahhaj, Koerner & Sargent 2007; HD 32297, Moerchen et al. 2007a; Fomalhaut, Stapelfeldt et al. 2004; ζ Lep, Moerchen et al. 2007b; Vega, Su et al. 2005; δ Vel (Gáspár et al. 2008, although note that this excess emission is thought to arise from interaction with the interstellar medium; see Section 4.6). The light blue line on all images is 100 AU unless otherwise indicated. The peak in emission at ~10 Myr comes from dust at 70 AU indicating that, unless these are protoplanetary disk remnants, these regions have been stirred by this time.

5.1.4. Early disk evolution. Evidence is also emerging from *Spitzer* surveys of young clusters on the early evolution of A-star debris disks. **Figure 8** shows the >3-Myr evolution of A-star 24-μm fractional excesses (Currie et al. 2008), which includes an increase in the upper envelope over 5–10 Myr (Hernández et al. 2006). The interpretation of upper envelopes is potentially fraught with observational biases, because it is determined not just by the distribution of fractional excesses in the sample, but also by the number of stars in the sample. Likewise the interpretation of fractions of stars with excess depends on the threshold of the different surveys. This problem is mitigated in the study of Orion OB1b (5 Myr) and OB1a (10 Myr) (Hernández et al. 2006), which contributes to the rise in **Figure 8**, because the A-star samples in the two clusters are of similar size (∼30), have a similar detection threshold, and have a similar fraction of stars with 24-μm excess ($38 \pm 3\%$ and $46 \pm 4\%$) that is also comparable to that found by Rieke et al. (2005) at this age. However, the detection threshold in the study of h and χ Persei (13 Myr) ($R_\nu > 5-25$; Currie et al. 2008) means that only the brightest 1.7% of disks were detectable (from a sample of ∼1000). A similar threshold applies to the study of Sicilia-Aguilar et al. (2006), which found a similar fraction of bright excesses toward Tr37 (4.2 Myr, $6.9 \pm 3.4\%$) and NGC 7160 (11.8 Myr, $4.4 \pm 2.5\%$), which are also plotted in **Figure 8**. Sources with this level of excess in OB1b or OB1a are unlikely owing to the small sample size.

Nevertheless, the claim that sources with $R_\nu > 5-15$ at 24 μm are more common at 10–15 Myr than at 5 Myr (Currie et al. 2008) seems to be justified. Because few A stars are thought to have protoplanetary disks by 5 Myr, it is unlikely that the scheme used to classify a star as having a debris disk affects this result, although it is notable that **Figure 8** excludes protoplanetary disks with near-IR excesses, such as 5-Myr HD 290543, which lies in the otherwise unpopulated high 24-μm excess region at <10 Myr (Hernández et al. 2006), as does the transitional/debris disk of HD 141569.

A high fraction of A stars with $R_\nu > 5$ excesses at 24 μm is also seen in the 8-Myr TW Hya association (1/1 = 100%, Low et al. 2005), and in the 12-Myr β Pic association (3/5 = 60%; Telesco et al. 2005, Chen et al. 2006). However, because the combined rate for these two associations, 4/6 = 67%, is much higher than that of 1.7% reported for 13-Myr h and χ Persei (Currie et al. 2008), this introduces the complicating possibility that early disk evolution could be affected by cluster environment, although the detection rate in h and χ Persei would have to be measured down to a uniform threshold of $R_\nu > 5$ before anything can be concluded from such a comparison. It is not known whether the evolution of protoplanetary disks is environment dependent. Although there are several isolated 5- to 10-Myr Herbig Ae stars (Mannings & Sargent 1997; **Figure 3**), these are significantly biased samples and so are not representative of the frequency of long-lived disks.

5.1.5. Interpretation of the 10- to 15-Myr peak. The peak at higher fractional excesses at 10–15 Myr is interpreted as evidence for self-stirring. However, this interpretation is not as straightforward as implied by the evolutionary tracks on **Figure 8**, because these show only the evolution of 30- to 150-AU material in self-stirring models. A lack of high-excess sources at <10 Myr in this model requires the inner 30 AU of the majority of A stars to have been cleared of planetesimals through some mechanism other than self-stirring by the time the protoplanetary disk disperses (see **Figure 5** and Section 4.3). As yet, little is known about <30 AU disks, should they exist, because their short collisional lifetimes mean that they would not last long above the detection threshold (**Figure 7**). The lack of high-excess sources at <10 Myr also implies that disks that are bright at 10–15 Myr were fainter at earlier times (unless they are descendants of HD 141569-like disks), which would also explain the lower (15%) fraction of stars with debris disks found at 3 Myr (Hernández et al. 2007a). This can be explained in a consistent manner with a delay of 10 Myr until the onset of stirring.

Two of the disks that are at the peak in 24-μm excess, HR4796 and β Pic, have been resolved in the mid-IR (Telesco et al. 2000, 2005), showing where this emission comes from in this phase (see **Figure 8**). Although the 24-μm flux for β Pic arises from dust at distances of 20–120 AU, that seen toward HR4796 is narrowly confined at 70 AU. Both are inferred to have planetesimal belts at ∼70 AU that have been stirred by ∼10 Myr. Self-stirring models predict that to grow 2000-km objects at 70 AU in 10 Myr requires a surface density that is $20 \times$ MMSN (Equation 12), which is at the high end of the protoplanetary disk mass distribution (Andrews & Williams 2007). Either massive protoplanetary disks are atypically common in these associations or planet formation models need to achieve an order-of-magnitude-faster growth.

5.1.6. Relation with planets. Stirring by giant planets closer to the star (Section 4.3) may be another way of stirring a 70-AU disk in 10 Myr. Evidence for a 2-$M_{\rm Jup}$ planet at 10 AU has already been suggested around β Pic from red-shifted variable absorption features (Beust & Morbidelli 2000) and from a warp in the dust disk structure (Augereau et al. 2001). An inner planetary system would also explain the inner clearing (Freistetter, Krivov & Löhne 2007; Faber & Quillen 2007). The outward migration of smaller, Neptune-mass planets could also stir up the disk at 70 AU and clear the inner regions. Evidence for such evolution may lie in the detailed structure of some older disks. For example, the clumpy structure in Vega's submillimeter disk (Holland et al. 1998) can be explained by the outward migration from 40–65 AU of either a Neptune-mass planet over 56 Myr (Wyatt 2003), or of a 2-$M_{\rm Jup}$ planet from 40–65 AU over 0.3 Myr (Martin et al. 2007). Such migration processes could be ongoing in systems such as β Pic and HR4796 (Section 4.4). Although debris disks provide indirect evidence for the architecture of A-star planetary systems (Wyatt et al. 1999; Wyatt 2005b, 2008; Quillen 2006), radial velocity surveys are also finding a relatively high frequency of giant planet detections around evolved A stars on the post-main sequence (Johnson et al. 2007), suggesting that the formation of giant planets may be a common occurrence around A stars. Imaging surveys for planets at larger distance have yet to restrict possible scenarios for debris disk evolution, although they have ruled out >7-$M_{\rm Jup}$ planets at >20 AU from Vega (Hinz et al. 2006).

5.1.7. Protoplanetary disk remnants. To ascertain whether the high excess ratio of systems like β Pic and HR4796 arise from protoplanetary disk remnants (Sicilia-Aguilar et al. 2006; Section 3.2), a knowledge of the gas content in these systems is essential, because this affects the correspondence of the dust distribution with that of the planetesimals. Although gas is seen toward β Pic (Brandeker et al. 2004), it is thought that this gas is not a remnant of the protoplanetary disk, but produced in planetesimal collisions (Czechowski & Mann 2007), planetesimal sublimation (Beust & Valiron 2007), or photon-stimulated desorption (Chen et al. 2007). This gas reacts differently to radiation pressure compared with expectation (Brandeker et al. 2004), which can be explained by the carbon abundance of the gas (Roberge et al. 2006) that allows the gas to be self-braked, or braked by the dust (Fernández, Brandeker & Wu 2006), although the origin of the high-carbon abundance still remains to be understood. This gas, and any left over from the protoplanetary disk, may also affect the grain dynamics (Section 3.2), and although no gas is seen toward HR4796 (Chen & Kamp 2004), this does not rule out gas-dust interactions causing confinement of the dust to a ring, because these interactions operate even with relatively small quantities of gas (Besla & Wu 2007, Beust & Valiron 2007). Three other bright young A/B-star debris disks also have a circumstellar gas component (HD 141569 at 5 Myr, Jonkheid et al. 2006; 49 Ceti at 8–20 Myr, Dent, Greaves & Coulson 2005; HD 32297 at <30 Myr, Redfield 2007; see **Figure 8**), indicating that a gaseous component is either necessary for, a by-product of, or coincidental with (due to the young age of both phenomena) high dust excess.

It is also possible to set some constraints on a protoplanetary origin for the dust from a consideration of its collisional lifetime, because putting $D_c = 10^{-6}$ km into Equation 16 shows that a belt of <1 mm dust at $f = 10^{-3}$ at 70 AU from an A0 star only lasts a few thousand years (see also Wyatt et al. 1999). This argument implies that dust seen in HR4796 must be replenished from larger grains, which would themselves be unaffected by gas drag. One way around this would be for collisions not to be destructive, perhaps because relative velocities have been damped by remnant gas. Low (albeit destructive) relative velocities in the HR4796 disk have also been suggested from its sharp outer edge (Thébault & Wu 2008). This reinforces the importance of working out how much gas is in these young debris disk systems, and of ascertaining how that affects the dust dynamics.

5.2. FGK Stars

The debris disks of sun-like stars have been studied using 24 μm, 70 μm, and submillimeter surveys, as well as optical imaging. The 24-μm results show a qualitatively different behavior to that seen at longer wavelengths, and so are discussed separately here.

5.2.1. ≤24-μm evolution. A debris disk of a sun-like star must have a radius ≪30 AU to exhibit a detectable 24-μm excess in a survey that is calibration-limited to $R_{\nu\,\text{lim}} = 0.1$ (**Figure 1**). Surveys with IRAS showed that such mid-IR excesses are rare (Aumann & Probst 1991, Gaidos 1999), a finding confirmed with ISO (Laureijs et al. 2002), the *Midcourse Space Experiment* (MSX; Uzpen et al. 2007) and *Spitzer* (Bryden et al. 2006, Hines et al. 2006). For field stars with a median age of ~5 Gyr, the detected fraction in *Spitzer* surveys is ~4% (Trilling et al. 2008). However, surveys that focus on young sun-like stars (Chen et al. 2005, Siegler et al. 2007, Meyer et al. 2008) have shown that, just as for A stars, the 24-μm statistics are a strong function of age. The fraction of FGK stars with 24-μm excess falls with time from 20% to 40% at the youngest ages to a few percent on a 10-Myr timescale (see **Figure 9**). The exact shape of the fall-off remains debatable; Meyer et al. (2008) suggest a sharp drop at 300 Myr, although a linear fall-off with time is consistent with the data. The fall-off mimics that of A stars, except on a timescale that is an order-of-magnitude shorter for sun-like stars. This difference in timescale, combined with the longer main sequence lifetime of sun-like stars, goes some way to explaining the rarity of 24-μm excesses around field FGKs. No formal difference is seen between the excess fractions of open clusters and field stars (Meyer et al. 2008), indicating that there is no strong dependence of disk evolution on star-forming environments.

---→

Figure 9

Evolution of 24-μm excesses around sun-like stars (Siegler et al. 2007). (*a*) 24-μm excess ratio as a function of age (noting that it is $R_\nu + 1$ that is plotted here). Dust seen in systems like HD 23514, BD+20307, HD 69830, and η Corvi stands out above the envelope of fractional luminosity versus age. This dust component is thought to be transient, and so these systems revert to lower quiescent levels on a timescale that is much shorter than the system age; i.e., there is a significant stochastic element to this evolution on top of an underlying fall-off with age. Stochasticity could result from dust input from a recent collision or a recent dynamical instability. (*b*) Fraction of stars with 24-μm excess as a function of age. Filled circles show the results for FGK stars, whereas squares are those for A stars (Siegler et al. 2007). The sun-like star results of Meyer et al. (2008) in different age bins are shown in red, whereas the results for sun-like stars in clusters and associations of different ages are shown in orange (Siegler et al. 2007). The evolution of FGK emission mimics that of A stars except that it is an order of magnitude faster. This can be explained by either steady-state processing of asteroid belts or dust produced during terrestrial planet formation.
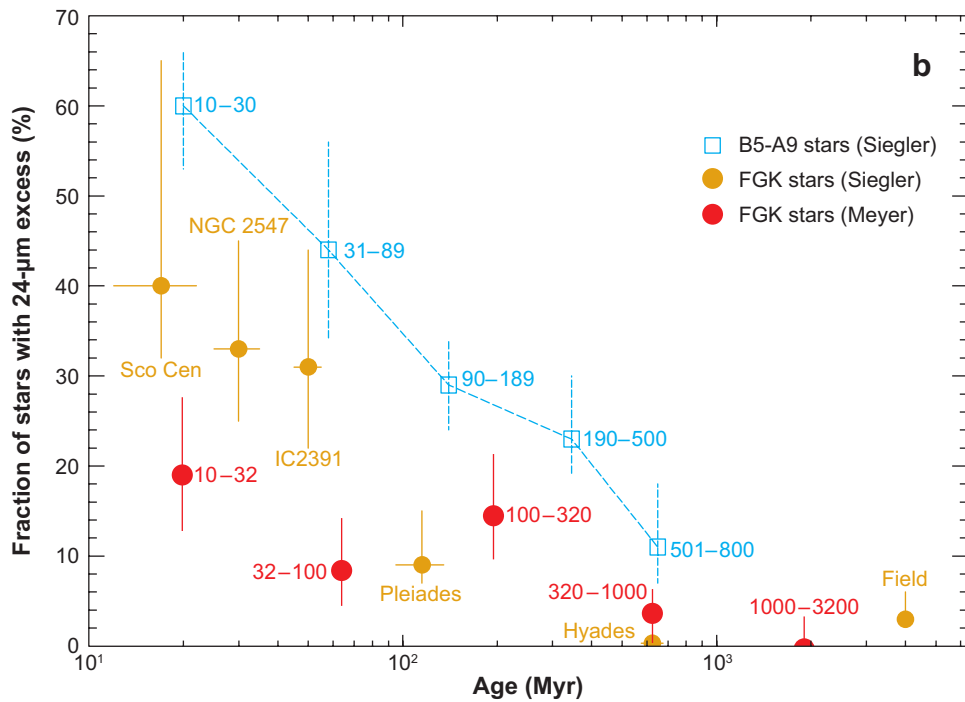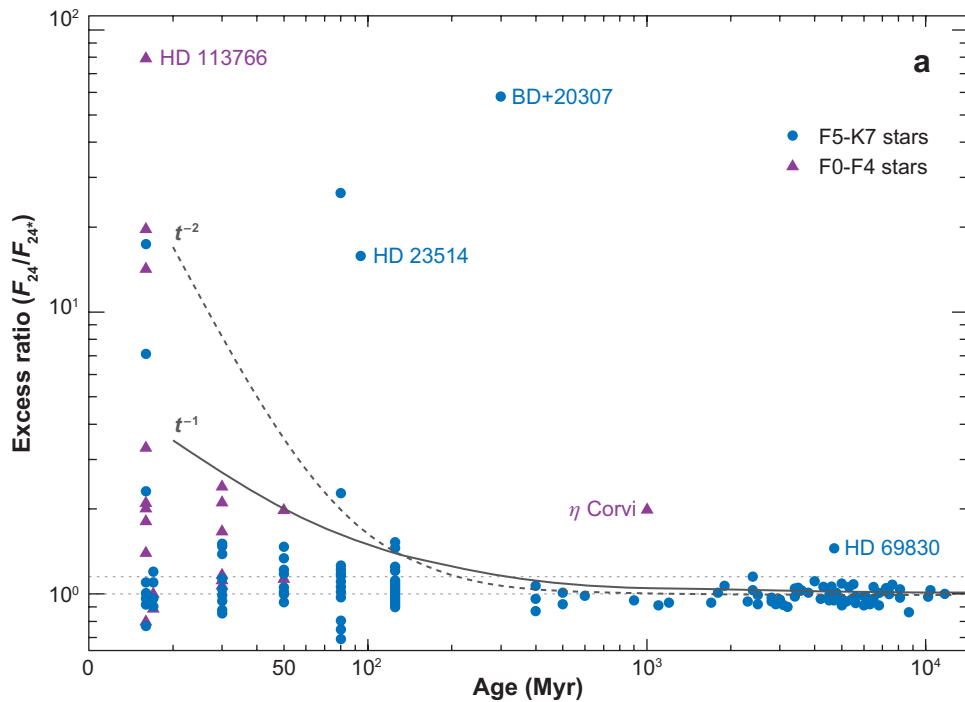
5.2.2. Terrestrial planet formation versus asteroid belt. A 100-Myr timescale for the decay in 24-μm excess corresponds well with that expected for excess emission created during terrestrial planet formation (Kenyon & Bromley 2004b), as well as with the timescale for the final accretion of the Earth (Halliday & Kleine 2006). Thus it is plausible that we are witnessing terrestrial planet formation in action in these systems, either the grinding away of the <100-km planetesimal population following the formation of 2000-km planetesimals or the products of massive protoplanet collisions (Siegler et al. 2007, Meyer et al. 2008). If so, these observations provide valuable constraints on terrestrial planet formation processes. However, because the A-star 24-μm statistics can be explained by steady-state evolution of prestirred planetesimal belts (Wyatt et al. 2007b), it is also possible that we are witnessing collisional grinding of the asteroid belts of these stars. This is supported by the fact that the order-of-magnitude-faster fall-off for the planetesimal belts of FGK stars compared to those of A stars is predicted by steady-state evolution models: Although the disks of FGK stars have to be seven times closer to the star to reproduce the same dust temperature (Equation 3), the disks of A stars can be detected down to a four times lower fractional luminosity for an equivalent calibration-limited detection threshold (Equation 11), which translates into a timescale for such disks to disappear that is 20 times shorter for FGK-star disks than for A-star disks (Equation 16).

Detailed studies of young disks detected at 24 μm may help to distinguish between the two interpretations. However, the levels of hot dust seen around HD 98800 (8 Myr) at 3.4 AU (Akeson et al. 2007), HD 113766 (16 Myr) at 1.8 AU (Lisse et al. 2008), and HD 12039 (30 Myr) at 5 AU (Hines et al. 2006) are in line with those expected from steady-state processing (Equation 18; Wyatt et al. 2007a), meaning that the asteroid belt interpretation cannot be easily ruled out. The infrared spectrum of HD 113766 is also not useful to distinguish between the interpretations, however the inferred asteroidal (rather than cometary) composition of the dust has the potential to provide constraints on the mechanism and location for the formation of the parent bodies of the dust (Lisse et al. 2008).

Regardless of the origin of the 24-μm emission, its high incidence rate of 20–40% at young ages implies that growth to >1-km planetesimals close to sun-like stars is a common occurrence. Because asteroid belts decrease in brightness in the steady-state evolution model, this statistic could imply that ∼1/3 stars have a planetesimal belt <30 AU. Meyer et al. (2008) perform a similar analysis for the terrestrial planet-formation interpretation and suggest that, because 24-μm flux in the models undergoes peaks and troughs (**Figure 4**), and not all systems with ongoing formation exhibit excess emission at any one time, it may be possible to sum fractions in different age bins to infer that 60% of stars form terrestrial planets.

5.2.3. Transient hot dust. Neither the terrestrial planet-formation models of Kenyon & Bromley (2005), nor the asteroid belt interpretation can explain the presence of hot dust around >100-Myr stars such as η Corvi (Wyatt et al. 2005), BD+20307 (Song et al. 2005), HD 69830 (Beichman et al. 2005), HD 72905 (Beichman et al. 2006b), and HD 23514 (Rhee, Song & Zuckerman 2008) (see **Figure 9a**). The abnormality of such sources can be quantified by comparing the ratio of observed fractional luminosity to the maximum expected from steady-state asteroid belt evolution (Equation 18). Using the parameters for A-star belts shows that these disks have $f > 1000 f_{max}$ (Wyatt et al. 2007a; see also Löhne, Krivov & Rodmann 2008) and so cannot be explained by steady-state planetesimal belts colocated with the dust, as the processing timescales are so short compared with the stellar age that the dust from such belts would have already been depleted below a detectable level. Two possible origins for the hot dust have been proposed; either it is transient dust from a recent collision between two growing protoplanets or two large planetesimals in an asteroid belt (Song et al. 2005; Rhee, Song & Zuckerman 2008; Section 4.2), or it is derived from

a planetesimal belt further from the star where the mass required to sustain the inferred mass-loss
rate can survive for ≫100 Myr (Wyatt et al. 2007a).

5.2.4. Recent collision versus outer belt origin. Although a collisional origin for the dust
agrees with our understanding of planet-formation processes and of Solar System evolution, there
is a timescale problem in that steady-state evolution should have reduced planetesimal belt mass
such that massive collisions are infrequent by 100 Myr (Wyatt et al. 2007a). Debris produced in
such events is short-lived, resulting in a low probability of witnessing collisions between massive
asteroids. This problem may be mitigated by the relatively slow evolution of planetesimal belt
mass in more detailed models (Löhne, Krivov & Rodmann 2008). The frequency of protoplanet
collisions and the duration of the resulting dust debris need to be quantified by the models to
assess this interpretation of the observations, although a simple estimate of the lifetimes of frag-
ments feeding the dust seen toward the youngest systems, HD 23514 (100 Myr) and BD+20307
(400 Myr), suggests that catastrophic disruption of planetary embryos may be a viable explanation
(Rhee, Song & Zuckerman 2008).

For two of the systems with hot dust there is evidence at longer wavelengths for material
further from the star (Wyatt et al. 2005 Beichman et al. 2006b). This type of system is exempli-
fied by η Corvi, which has both a planetesimal belt imaged in the submillimeter at 100–150 AU
(Wyatt et al. 2005) and a hot dust component constrained by unresolved mid-IR imaging that is
<3.5 AU (Smith, Wyatt & Dent 2008). The fraction of hot dust sources detected at 70 μm (2/4)
is not significantly higher than the 16% of all stars that harbor 70-μm excesses (Bryden et al.
2006, Trilling et al. 2008). However, if the 70-μm excess of HD 23514 was confirmed, the pos-
sibility of a correlation may need to be reconsidered (Rhee, Song & Zuckerman 2008). Near-IR
interferometry has also resolved a hot dust component <0.1 AU from the star τ Ceti (di Folco
et al. 2007), which also hosts an outer disk of radius 55 AU (Greaves et al. 2004b; see **Figure 10**).
Given its 10-Gyr age, the hot dust of τ Ceti cannot originate in a planetesimal belt at ≪1 AU and
may have its origin in the outer disk. Nevertheless, the nondetection of long-wavelength excess
toward HD 69830 above that expected from the hot dust also indicates that a cold dust reservoir is
not necessarily required for a hot dust excess (Beichman et al. 2005, Trilling et al. 2008). However,
evidence for a connection of the hot dust with planetesimals formed at greater distance in this
system may be found in its infrared emission spectrum, which suggests a dust composition similar
to P- and D-type asteroids and a component of water ice (Lisse et al. 2007).

The way in which planetesimals in these systems might be scattered in from further out is not
clear, nor is it clear whether this happened recently or soon after or during the protoplanetary
disk phase. We may be witnessing systems undergoing a dynamical instability (Section 4.4), i.e., a
late heavy bombardment-type event (Wyatt et al. 2007a). Other possibilities are that a 2000-km
icy planetesimal has been captured in a circular orbit at 1 AU, or that these planetesimals are
scattered in like the comets in the Solar System (Section 4.5), although it remains to be explained
how to achieve systems with 10^6 Hale Bopp-type comets (Beichman et al. 2005) except through
a dynamical instability. The clue to the origin of the excess in HD 69830 may be in its planetary
system, which is comprised of three Neptune-mass planets within 0.7 AU (Lovis et al. 2006), and
in its formation in which the outermost planet is thought to have migrated in from 8 AU (Alibert
et al. 2006); the consequences for the remnant planetesimal belt in this scenario have yet to be
explored.

5.2.5. ≥70-μm evolution. The fraction of stars with detectable 70-μm excess is ~16%
(Beichman et al. 2006a, Bryden et al. 2006, Trilling et al. 2008). The majority of the 225 stars in
these observations had a detection threshold of around $R_{\nu\,lim} \approx 0.55$, although observations of
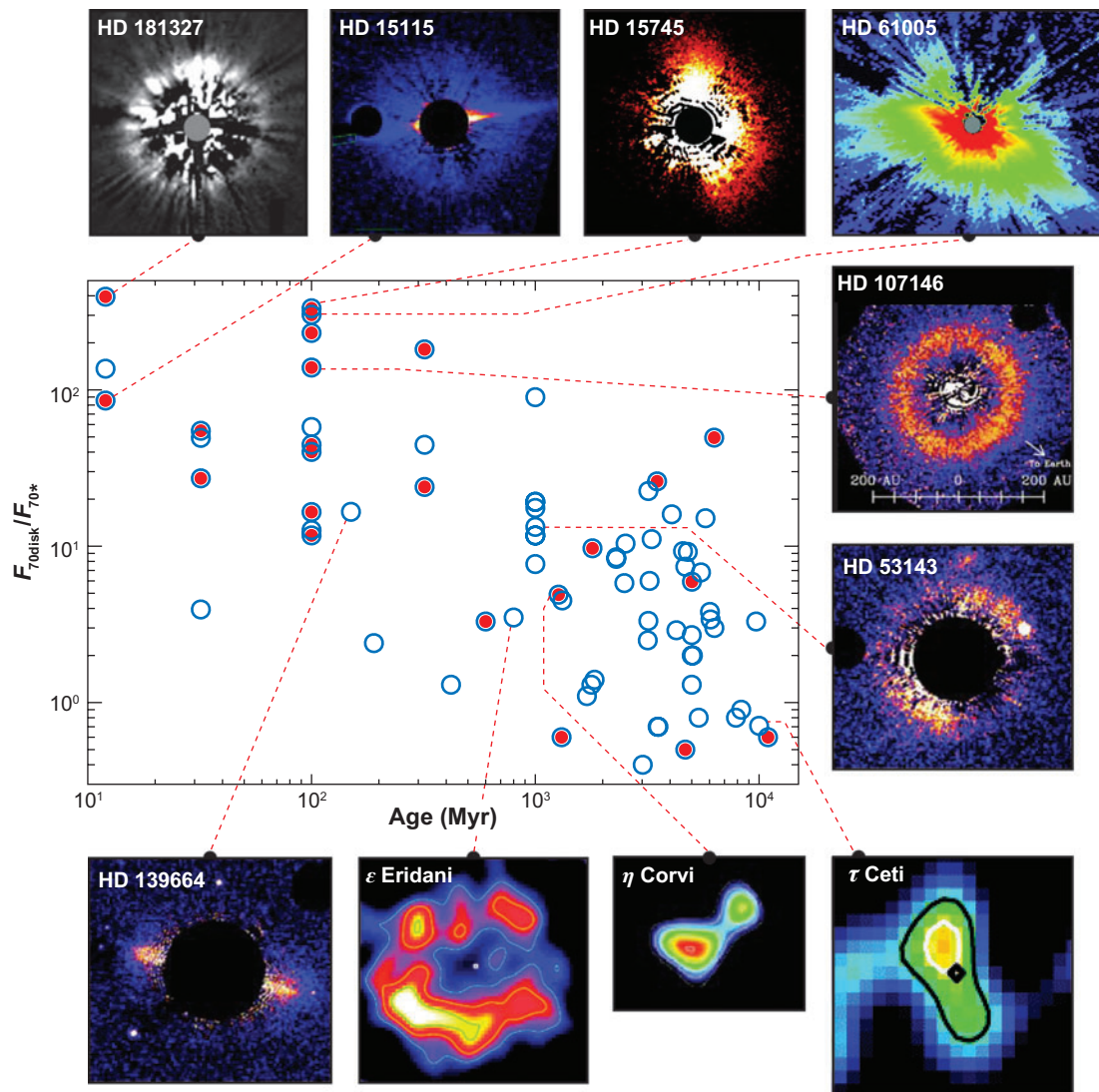
Figure 10

Evolution of 70-μm fractional excess for sun-like stars (Habing et al. 2001, Beichman et al. 2006a, Moór et al. 2006, Hillenbrand et al. 2008, Trilling et al. 2008). Stars with excess emission also detected at 24 μm are shown with filled red circles. Images of individual disks are highlighted to illustrate the origin of the emission as a function of age. Images are of scattered light for HD 181327 (Schneider et al. 2006), HD 15115 (Kalas, Fitzgerald & Graham 2007), HD 15745 (Kalas et al. 2007), HD 61005 (Hines et al. 2007; see Section 4.6), HD 107146 (Ardila et al. 2004), and HD 139664 and HD 53143 (Kalas et al. 2006). Images are of submillimeter emission for ε Eridani (Greaves et al. 2005), η Corvi (Wyatt et al. 2005), and τ Ceti (Greaves et al. 2004b). The slow fall-off with age can be explained by steady-state processing (Löhne, Krivov & Rodmann 2008), although this does not rule out a role for delayed stirring in debris disk evolution.

the more distant stars did not reach this level. As expected, a lower fraction with excess is seen in surveys in which a larger number of targets are sensitivity limited (~10% of the 328 targets in Hillenbrand et al. 2008 were found to have excess). It is debatable whether there is a dependence on spectral type within the FGK spectral-type range. Although the fraction of stars with excess decreases across spectral types A-M, it could be constant within the FGK range (Bryden et al.

2006, Trilling et al. 2008), although a lower excess rate is found for late-type stars greater than K1 (Beichman et al. 2006a, Hillenbrand et al. 2008, Trilling et al. 2008). Given the observational bias that fractional luminosities must be higher around later spectral types to be detected (see **Figure 1**; Gautier et al. 2007), the observed lack of spectral-type dependence is somewhat surprising. However, this bias is modulated by the (unknown) radius distribution, which may have a spectral type dependence, and is offset to some degree by the higher ratio of fractional luminosity to mass expected for lower mass stars (Equation 15). For now, at least, it seems appropriate to use an FGK umbrella for sun-like stars.

The 70-μm excesses of sun-like stars persist for longer than those at 24 μm, and are found up to 10 Gyr (Hillenbrand et al. 2008, Trilling et al. 2008). Although the median age of stars with 70-μm excess is younger than average (2.6 Gyr compared with 4.3 Gyr; Bryden et al. 2006), the excess rate is also consistent with a flat evolution for 0–10 Gyr (Hillenbrand et al. 2008, Trilling et al. 2008). **Figure 10** shows the evolution of $F_{70\,\mathrm{disk}}/F_\star$ for the disks detected around sun-like stars. [Surveys have typically plotted this information by converting the measured $F_{70\,\mathrm{disk}}/F_\star$ into a fractional luminosity f using some assumption about disk temperature, e.g., that it is as hot as it could be without being detected at 24 μm. Although this introduces a bias into this representation of the observations, it is not one which has affected our interpretation of disk evolution, because that inferred from studies of (biased) f show similar features to that inferred from $F_{70\,\mathrm{disk}}/F_\star$.] It is found that: (*a*) the upper envelope in 70-μm flux decreases very slowly with age, (*b*) there is a large spread in excess at each age, and (*c*) there is a lack of young sources with low excess ratios.

Most of these features are also seen in ISO (Decin et al. 2003) and IRAS (Rhee et al. 2007) studies, and similar features can be seen in the evolution of submillimeter dust masses for FGK stars for which the upper envelope is reasonably flat at ∼0.1 $M_\oplus$ (**Figure 3**). There are some observational biases to consider when assessing **Figures 3** and **10**. For example, the decrease in the lower envelope of dust mass with time, shown in **Figure 3**, may be attributable to the fact that nearby stars, for which it is possible to detect less massive disks, tend to be older; the lowest dust mass is detected around 10-Gyr τ Ceti at 3.65 pc (Greaves et al. 2004b). Because the nearest star younger than a given age is likely to be at larger distance for younger ages this introduces a $t_{\mathrm{age}}^{-2/3}$ fall-off in the lower envelope for a sensitivity-limited survey. The lower envelope of 70-μm excesses may have a similar origin (Rhee et al. 2007).

5.2.6. Steady-state interpretation. The features of the 70-μm evolution of sun-like stars can all be explained by the simple steady-state evolution models of Section 4.1, because a relatively slow fall-off with time is expected if most planetesimal belts detected at 70 and 850 μm have yet to reach collisional equilibrium, e.g., because their radii are ≫30 AU (see **Figure 5a**; Wyatt et al. 2007b). A slow fall-off is also expected in more detailed steady-state evolution models when the increase in planetesimal strength with size for $D > 1$ km is accounted for, and Löhne, Krivov & Rodmann (2008) showed that a suitable range of planetesimal belt initial masses ($0.01 - 30\,M_\oplus$) and radii (20–120 AU, where $dr/r = 0.5$) can be chosen to match the observed excess ratio distribution at all ages. The nondetection at 70 μm of 84% of stars in this scenario could mean that just 16% of FGK stars are born with massive planetesimal belts, although it may be possible to reduce the fraction of diskless stars with suitable distributions of initial masses and radii (Bryden et al. 2006). However, it can be inferred that the fractional luminosities of sun-like star disks are concentrated at lower values than those of A stars, because 70-μm observations of sun-like stars probe the same region of fractional luminosity versus radius parameter space as 24-μm observations of A stars (see **Figure 1**), yet half as many disks are detected in this region for sun-like stars than for A stars (see also Greaves & Wyatt 2003). Because sun-like star disks are expected to have higher luminosities

for a given mass (Equation 15), this implies that their disks are also on average less massive than those of A stars.

A significant unknown in this interpretation is the fraction of disks detected at 24 μm that can be attributed to steady-state evolution of >10-AU belts. It is suggested that the 24- and 70-μm emission of sun-like stars arises from two distinct regions (Gorlova et al. 2006, Trilling et al. 2008). Although 24/70-μm and 33/70-μm flux ratios indicative of 5- to 30-AU disks are seen (Beichman et al. 2006b, Hillenbrand et al. 2008, Trilling et al. 2008), high-resolution studies are required to determine whether these temperatures are instead caused by a combination of a belt at <5 AU and another at >30 AU (as is the case for η Corvi; Smith, Wyatt & Dent 2008) or if the hot temperatures are caused by small dust grains in a more distant belt that are heated above black body temperatures (as is the case for HD 181327; Schneider et al. 2006) (see **Figure 10**).

5.2.7. Constraints on delayed stirring models. The delayed stirring model also exhibits a slow fall-off in fractional excess with time (**Figure 5b**) and so may explain the observations (Dominik & Decin 2003). Although observations give no indication of disk radius increasing with age (Najita & Williams 2005), this finding cannot rule out the delayed stirring model, because any increase is predicted to be slow ($r \propto t_{age}^{1/3}$ from Equation 12). One crucial test of the delayed stirring model may come from the surface density profiles of individual disks (Section 4.3). In particular, a prestirred model would predict a shallow increase in density with radius $\propto r^{7/3}$, with a slightly steeper increase for self-stirred models. This could lead to appearance as a broad ring (see **Figure 10**), and may explain why some systems cannot be fitted with a single temperature spectrum (e.g., Hillenbrand et al. 2008). Kalas et al. (2006) noted that the disks of HD 53143 (1 Gyr) and HD 107146 (100 Myr) are seen to be wider than 50 AU. The inner edge of the HD 107146 disk (**Figure 3** of Ardila et al. 2004) could be consistent with a $r^{7/3}$ slope; its 130-AU radius is also consistent with self-stirring for an initial surface density of $10 \times$ MMSN (Equation 12). A broad ring morphology is also seen for HD 15115 (12 Myr, Kalas, Fitzgerald & Graham 2007) and HD 15745 (~100 Myr, Kalas et al. 2007). Detailed analysis of the radial distribution of dust in these systems, and its implications for the distribution of parent planetesimals (Wyatt 2008), is required to assess the possibility that these are self-stirred (or prestirred) extended planetesimal belts.

The radii of the disks of sun-like stars in the β Pic association may provide constraints on self-stirring models, because unless these are protoplanetary disk remnants or debris disks in which planet formation is ongoing, the stirring mechanism must be effective at the observed radius by 12 Myr. Equation 12 shows that the disks of HD 181327 (68–104 AU, Schneider et al. 2006), HD 15115 (31–554 AU, Kalas, Fitzgerald & Graham 2007), HD 164249 (27 AU, Rhee et al. 2007), and HD 191089 (11 AU, Smith, Wyatt & Dent 2008) could be self-stirred by this age given initial surface densities that are $30 \times$, $1 \times$, $1 \times$, and $0.1 \times$ MMSN, respectively, a distribution compatible with that observed for protoplanetary disks (Andrews & Williams 2005). The possibility that the disks of young sun-like stars are protoplanetary disk remnants is not as widespread in the literature as for young A-star disks, perhaps because gas has not been detected toward any sun-like star debris disks (Pascucci et al. 2006), although the issues raised in Section 3.2 apply equally to the disks of sun-like stars.

5.2.8. Relation with planets. An alternative stirring mechanism is the presence of planets that formed closer to the star (Section 4.3). There is as yet no evidence that detectable debris correlates with planets that are detectable in radial velocity surveys (Greaves et al. 2004a, Beichman et al. 2006a, Moro-Martín et al. 2007). Detectable debris also does not correlate with stellar metallicity, as does the presence of a detectable planet (Greaves, Fischer & Wyatt 2006; Beichman et al. 2006a). However, an emerging (albeit weak) correlation is that disks around stars

with planets have higher 70-μm excess ratios than those without planets (G. Bryden, C.A. Beich-man, K.R. Stapelfeldt, M.W. Werner, S.M. Lawler, et al., manuscript submitted). If confirmed, this may arise because the protoplanetary disks that form detectable planets are the most mas-sive in the distribution, and such massive disks would also, on average, have more massive debris disks (Wyatt, Clarke & Greaves 2007). This would imply that the known planets do not influ-ence the evolution of the known debris disks, which is not surprising because planets are found at <5 AU and disks are found at >30 AU, but the two phenomena are connected through the initial conditions of the protoplanetary disk required to result in either detectable planets or de-bris (Section 3). However, similar to the disk of HD 38529 (Moro-Martín et al. 2007), the disk at 60 AU from ε Eridani (Greaves et al. 2005; **Figure 10**) is expected to have been influenced to some extent by the secular perturbations of the 0.8-M_{Jup} planet at 3.4 AU (Benedict et al. 2006) on a timescale (∼100 Myr; Wyatt 2005b) that is shorter than the 800-Myr age of the system. Systems with both disks and planets are becoming more common (the current tally is 10), and will undoubtedly increase our understanding of the effect of planet-disk interactions on debris disk evolution.

5.2.9. Implications for Solar System evolution. One of the goals of studying debris disk evo-lution is to place the Solar System into context (Meyer et al. 2007). Comparing the five nearest sun-like stars to the Earth with each other shows that the Solar System is not atypically dusty, because both ε Eridani and τ Ceti fall within this sample and exhibit >20 times more dust than the present Kuiper belt (Greaves et al. 2004b). However, it is not yet possible to infer an atyp-ically low dust content for the Solar System, because a Kuiper belt analog around a distant star ($f ≈ 10^{-7}$, $M_{disk} < 2 × 10^{-5} M_⊕$, $r = 40$ AU) would not be detectable (see **Figures 1** and **3**). Because the Kuiper belt's low mass may be caused by depletion in a dynamical instability (Section 4.4; Gomes et al. 2005), it should have been detectable prior to that instability, which may have occurred as late as 800 Myr (Stern 1996, Meyer et al. 2007; M. Booth, manuscript in preparation; **Figure 5c**). During this early epoch, the models predict that there was ∼30 $M_⊕$ of material at ∼25 AU that would result in a 70-μm excess ratio of ∼50 (Equations 10 and 15; see **Figure 10**). Because there is no significant deficit of old systems with 70-μm excess this could indicate that the Sun is one of ∼16% of sun-like stars with a bright debris disk at young ages, but is among a small fraction of such systems that undergo an instability that depletes its debris disk. Also, because the models of Gomes et al. (2005) and Thommes et al. (2007) have a Kuiper belt inner edge at 15–20 AU in the first 800 Myr, the debris disk of the young Sun might have been detectable at 24 μm; the 24-μm excess ratio is marginally detectable at ∼0.1 for the above parameters (see **Figure 9**). Models for the evolution of the Solar System, and of planet formation more generally, should routinely make predictions for the resulting infrared luminosity for comparison with debris disk statistics.

5.3. M Stars

M stars are intrinsically interesting because they comprise ∼70% of the total number of stars in the Galaxy. However, only a small fraction of these stars are known to host debris disks. In a cross-correlation of the Hipparcos catalog with IRAS, Rhee et al. (2007) found just one M star out of 900 with excess. That star is 12-Myr M1V AU Mic, which is in the β Pic association, and its edge-on disk has been imaged showing dust in projected separation from 10–210 AU (Fitzgerald et al. 2007), consistent with dust produced in a planetesimal belt at 43 AU (Strubbe & Chiang 2006). Other researchers have used the IRAS catalogs to identify excesses at 12 and/or 25 μm toward M stars that have subsequently been ruled out from ground-based photometry (Song et al. 2002;

Plavchan, Jura & Lipsky 2005), a finding attributed to false positives resulting from searching large catalogs. A low fraction of M stars with excess was also found in a *Spitzer* survey in which no excess was found at 24 μm for 62 stars (to $R_{\nu\,\mathrm{lim}} = 0.3$) or at 70 μm for 20 stars (to $R_{\nu\,\mathrm{lim}} = 1$) (Gautier et al. 2007). However, small number statistics means that the incidence rate at 70 μm (<14% with 2σ confidence) could be similar to that of sun-like stars, and that M stars could have the same fractional luminosity distribution as FGKs (Gautier et al. 2007). Searches of young associations have been more fruitful, and three M-star disks (out of 18 M stars searched) were found at 24 μm in the 8-Myr TW Hydra association, TWA7, TWA13, and Hen 3–600 (Low et al. 2005; Matthews, Kalas & Wyatt 2007). Submillimeter surveys have also been successful, with excess emission seen toward 20–150-Myr GJ182 (Liu et al. 2004; B. Matthews, private communication) and 200-Myr GJ842.2 (Lestrade et al. 2006), implying an excess fraction of 13% for the age range 20–200 Myr, which is comparable to that of sun-like stars. The submillimeter map of GJ842.2 is of note because emission is also seen up to 30 arcsec from the star (∼600 AU in projected separation at 20.9 pc), possibly indicating an atypically large and massive disk. The evolution of M-star submillimeter disk masses is shown in **Figure 3** on which the mass of GJ842.2 is that within 7 arcsec of the star (J.F. Lestrade, private communication).

The underlying debris disk population is hard to disentangle from these statistics. The low detection rate can be attributed in whole, or in part, to observational bias, because the region of parameter space carved out by both 24-μm and 70-μm surveys is small (**Figure 1**). Assuming a similar radius distribution for the debris disks of different spectral type, surveys at longer wavelengths are needed to probe the cooler temperatures expected for M-star disks (Matthews et al. 2007). The fact that M-star disks have preferentially been detected around young stars could indicate that some process is acting to decrease disk luminosity with time, which could mean that the largest planetesimals reach collisional equilibrium quickly in these disks. However, it is possible that planetesimal formation is inhibited around M stars, and that some of the dust seen around young stars is a remnant of the protoplanetary disk. Indeed, Hen 3–600 is classed as an optically thick protoplanetary disk (Low et al. 2005, Huenemoerder et al. 2007), and the spectral-type dependence of the persistence of protoplanetary disks suggests that the transition to debris disk could occur relatively late for M stars (Section 3). Planetesimal growth cannot always be inhibited, however. Whereas the detection rate of gas giant planets is lower for M stars than for higher mass stars (Johnson et al. 2007), planets that are typically of Neptune-mass did manage to form around some M stars (Bonfils et al. 2007).

The lack of excess around M stars has been suggested to originate in the enhanced stellar wind drag of late-type stars (Plavchan, Jura & Lipsky 2005). Stellar wind drag acts in a similar manner to P-R drag to make dust spiral in toward the star, and can act on shorter timescales if $(dM_{\mathrm{wind}}/dt)c^2 L_\star^{-1} > 1$ (Jura 2004). Thus, while P-R drag acts on longer timescales to collisions in detectable disks (Wyatt 2005a; Section 4.1), the dust evolution of low-luminosity M stars may be affected by their stellar winds. Stellar mass-loss rates are hard to estimate, but are inferred to be higher at young ages by up to 1000 times that of the current solar wind for both sun-like and M stars (Wood et al. 2002; Plavchan, Jura & Lipsky 2005). The consequence of this drag force is to remove small grains from the distribution, which essentially reduces the ratio f/M_{tot} by increasing the minimum grain size in the distribution above D_{bl} as assumed in Equation 15; that blow-out size is irrelevant for M stars in any case, because their radiation pressure cannot put grains of any size onto hyperbolic orbits (i.e., $\beta < 0.5$; see Matthews, Kalas & Wyatt 2007). In other words, this exacerbates the problem of M-star disk detectability evident in **Figure 1**, but it does not imply that M stars do not have planetesimal belts. It also means that once the largest planetesimals come to collisional equilibrium, the fractional luminosity evolution of M-star debris disks would be expected to follow a t_{age}^{-2} fall-off (Dominik & Decin 2003).

5.4. Constraints from Resolved Imaging

This review has concentrated on information about disk evolution obtained from photometric studies of debris disks. However, resolved imaging also provides important constraints.

The primary value of imaging is to confirm the interpretation of an infrared excess as originating in a circumstellar disk and to determine the disk's radius, which can be poorly constrained from the emission spectrum, particularly if there is dust present with a range of temperatures and distances from the star (Section 2.5). Images of the same disk at different wavelengths often show quite different radial profiles, and a significant success of the past few years has been to explain this within a unified model of steady-state dust production through collisions in a planetesimal belt (Wyatt et al. 1999, Augereau et al. 2001, Strubbe & Chiang 2006, Augereau & Beust 2006; see review in Wyatt 2008), because radiation forces cause dust of different sizes, which are probed by different wavelength observations, to have different radial distributions that can extend both interior and exterior to the parent planetesimal belt. Although this means that caution (and careful modeling) is required when interpreting disk images, because the dust location does not necessarily correspond with that of the parent planetesimals, it also means that the images provide valuable insight into the dust production mechanism. For example, although the images of the β Pic and AU Mic disks can be explained by steady-state dust production (Augereau et al. 2001; Strubbe & Chiang 2006), the inferred ratio of small to large grains in the Vega disk implies a stochastic evolution (Su et al. 2005). The radial profiles provide further information on the dynamical state of the collisional cascade, and it has been suggested that the diversity in the shapes of disk outer edges may be explained by the degree to which they have been stirred (Thébault & Wu 2008); the sharp outer edge of the HR4796 disk implies a low eccentricity of $e \approx 0.0035$. There is also a large diversity seen in the shapes of the inner edges (e.g., Ardila et al. 2004, Kalas et al. 2005), which may have its origin in the masses of planets truncating the inner edge (Quillen 2006) or in the way in which extended planetesimal belts are stirred (Section 4.3).

Perhaps the most surprising discovery from imaging has been that a large number of the disks are asymmetric, showing features such as warps (Heap et al. 2000), clumps (Greaves et al. 2005; see ε Eridani in **Figure 10**), offset centers of symmetry (Kalas et al. 2005), spirals (Clampin et al. 2003), and brightness asymmetries (Telesco et al. 2000; see HR4796 in **Figure 8**). In fact, it is exactly this set of features that is predicted to be manifested in debris disks if there are also planets orbiting the star, because their gravitational perturbations would be imprinted in the dynamical structure of the planetesimal belts and would affect the dynamical evolution of the dust. Different structures are expected depending on the orbital configuration of the planetary system. For example, planets on eccentric orbits impose spiral structure on young disks (Wyatt 2005b), which propagates through the disk so that at later times the disk has an offset center of symmetry that may be seen as a brightness asymmetry (Wyatt et al. 1999). Similarly, a planet on an inclined orbit sets up a warp that propagates through a young disk (Augereau et al. 2001), although warped disks may be static features in old multiple planet systems (Wyatt et al. 1999). Disk structures may also depend on the system's past history. For example, planet migration can result in planetesimals being trapped in the planet's resonances resulting in a clumpy disk (Wyatt 2003, Reche et al. 2008). Clumps may also arise in low mass disks from the migration of dust into resonances through P-R drag (Ozernoy et al. 2000, Kuchner & Holman 2003, Krivov et al. 2007).

Detailed dynamical models of planet-disk interactions have been developed to allow the observed structures to set constraints on the perturbing planets (see review in Wyatt 2008), and **Figure 11** summarizes the properties of the planets inferred from structures seen in debris disk images. Although there will continue to be uncertainty about the existence of these planets
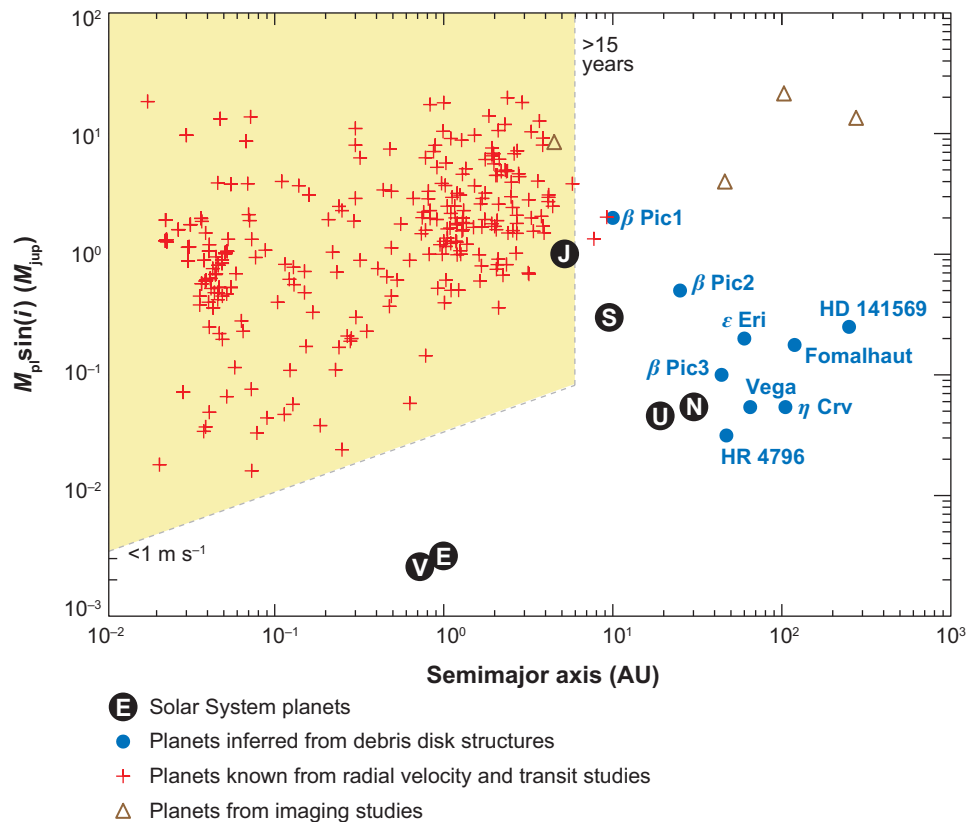
Figure 11

Distribution of planet masses and semimajor axes. Parameters for extrasolar planets found from radial velocity and transit and imaging studies were taken from **http://exoplanet.eu** on 31 January 2008. The shaded yellow region shows the current limits of radial velocity surveys for sun-like stars. Parameters for putative planets inferred from debris disk structures (which have yet to be confirmed) are from HR 4796, Wyatt et al. 1999; ε Eridani, Ozernoy et al. 2000; Vega, Wyatt 2003; HD 141569, Wyatt 2005b; η Corvi, Wyatt et al. 2005; Fomalhaut, Quillen 2006; and β Pictoris, Freistetter, Krivov & Löhne 2007. Note that these parameters, particularly planet mass, are often poorly constrained.

until they are confirmed using independent techniques, this figure illustrates how debris disks are probing an unexplored region of extrasolar planet parameter space inhabited by planets akin to Neptune in our own system. As well as having implications for planet-formation processes about where planets were able to form (or at least end up, see Martin et al. 2007) in these systems (Section 3.3), such planets may also explain how these debris disks were stirred (Section 4.3). Furthermore, the models required to explain some disk structures have implicit assumptions about the disk's past history, such as those requiring planet migration (Wyatt 2003; Section 4.4), or those in which structure propagates away from the planet (Augereau et al. 2001, Wyatt 2005b). For the majority of the observed asymmetric structures, unseen planets are the only explanation. However, it is possible that dust clumps in some young disks may arise from collisions between protoplanets (Sections 3.3 and 4.2). A close encounter with a nearby star has also been suggested as the origin of the extreme asymmetry in the HD 15115 disk (see **Figure 10**; Kalas, Fitzgerald & Graham 2007; Section 4.6).

6. SUMMARY AND FUTURE ISSUES

The observations presented in this review allow us to assess the relative importance of the different models for the evolution of the dust content of main sequence stars:

- **Steady-state evolution.** The steady-state collisional evolution of planetesimal belts is reasonably well understood. It appears that the majority of A stars, and some sun-like stars, have planetesimal belts that evolve in this way. The debris disk population thus sets important constraints on the outcome of planet-formation processes by providing information on how common planetesimal formation is in different parts of the protoplanetary disk. The steady-state evolution of dust from the planetesimal belts of M stars remains poorly constrained because of a lack of observational constraints and uncertainties in their stellar wind properties.

- **Stochastic collisions.** Steady-state evolution cannot explain all observed systems, some of which must have a stochastic component to their dust evolution. The origin and ubiquity of this stochasticity is unknown. Debris produced in single collisions may explain these observations, although simulations of dust produced in collisions between Mars-sized protoplanets would help assess this interpretation. The ignition of the collisional cascade could also be stochastic in some systems.

- **Delayed stirring.** Although most statistics can be explained by invoking planetesimal belts that are prestirred, the origin of the stirring has yet to be identified. Most stirring mechanisms require a delay between the birth of the star and the stirring of the planetesimal belt, and this is not ruled out observationally. Indeed a few results point to a role for delayed stirring in debris disk evolution, such as the peak in dust emission at 10–15 Myr for A-star disks. However, these observations also seem to require the inner 30 AU to have been cleared of planetesimals by the time the protoplanetary disk disperses. The stirring could come from within the belt (i.e., from the formation of 2000-km objects), and if we are witnessing planetesimal belts in which planet formation is ongoing, this would allow the assumptions of dust produced in this process to be tested. Stirring could also arise from gas giant or Neptune-sized planets formed closer to the star. A bigger inventory of systems with planets and debris is needed to determine the relationship between the two phenomena. The radial structure of debris disks provides a valuable diagnostic to distinguish between different interpretations.

- **Protoplanetary disk remnant.** To assess the possibility that ~10-Myr debris disks are protoplanetary disk remnants, more information is needed on the process of protoplanetary disk dispersal, and in particular on the quantity of gas that persists into the debris disk phase. Current upper limits to the gas content are not sensitive enough to rule out a significant role for gas in determining the dynamics of either debris disk or remnant dust.

- **Terrestrial planet formation.** The 24-μm emission of young sun-like stars may be a signature of ongoing terrestrial planet formation. However, it may equally be evidence for asteroid belts around the stars. Although knowledge of the distribution of planets in these systems would help to distinguish between these two interpretations, the detection of Earth-like planets is hard to achieve in the presence of dust (Beichman et al. 2006a). The composition of the dust inferred from analysis by way of its infrared spectrum may elucidate its origin.

- **Planetary system shake-down.** There remains considerable uncertainty about the origin of multiple-temperature debris disks with dust spanning several decades in offset from the star (0.1–100 AU). Transient events associated with dynamical instabilities during planetary system evolution may explain the unusual nature of some systems. However, the lack of evolution in the 70-μm statistics for sun-like stars beyond that expected from steady-state

processing suggests that such events are relatively rare. This could mean that the Solar System's evolution is atypical. Planet-formation models should consider debris disk statistics as serious constraints by routinely making predictions for the observability of debris in this phase.

Information about debris disk evolution from infrared photometry is complemented by that from imaging at wavelengths from optical to millimeter, which has provided crucial constraints on the dynamical state of the collisional cascade and on the stochastic nature of dust production. Imaging has also provided evidence that planets are orbiting within some disks through the discovery of asymmetries in their structures, and although these putative planets remain to be confirmed, the presence of planet-sized objects (i.e., bigger than Pluto) would naturally provide the stirring mechanism required for all debris disks (which otherwise has no explanation), and would further explain how the inner regions of these systems are cleared. Their formation mechanism could also plausibly reproduce the observed transient debris disk phenomena. Thus, although a connection between debris disks and planets remains to be conclusively proved, there exists a growing body of observations that is naturally explained with such a connection. Any alternative model must also explain these observations, and it is clear that debris disk studies will continue to play an integral role in the development of the planet-formation and protoplanetary disk evolution paradigms.

DISCLOSURE STATEMENT

The author is not aware of any biases that might be perceived as affecting the objectivity of this review.

LITERATURE CITED

Absil O, di Folco E, Merand A, Augereau J-C, Coude du Foresto V, et al. 2006. *Astron. Astrophys.* 452:237–44

Adams FC, Laughlin G. 2001. *Icarus* 150:151–62

Akeson RL, Rice WKM, Boden AF, Sargent AI, Carpenter JM, Bryden G. 2007. *Astrophys. J.* 670:1240–46

Alexander RD, Armitage PJ. 2007. *MNRAS* 375:500–12

Alexander RD, Clarke CJ, Pringle JE. 2006. *MNRAS* 369:229–39

Alibert Y, Baraffe I, Benz W, Chabrier G, Mordasini C, et al. 2006. *Astron. Astrophys.* 455:L25–28

Andrews SM, Williams JP. 2005. *Astrophys. J.* 631:1134–60

Andrews SM, Williams JP. 2007. *Astrophys. J.* 671:1800–12

Ardila DR, Golimowski DA, Krist JE, Clampin M, Williams JP, et al. 2004. *Astrophys. J.* 617:L147–50

Artymowicz P. 1997. *Annu. Rev. Earth Planet. Sci.* 25:175–219

Artymowicz P, Clampin M. 1997. *Astrophys. J.* 490:863–78

Asphaug E, Agnor CB, Williams Q. 2006. *Nature* 439:155–60

Augereau J-C, Beust H. 2006. *Astron. Astrophys.* 455:987–99

Augereau J-C, Nelson RP, Lagrange AM, Papaloizou JCB, Mouillet D. 2001. *Astron. Astrophys.* 370:447–55

Aumann HH, Beichman CA, Gillett FC, de Jong T, Houck JR, et al. 1984. *Astrophys. J.* 278:L23–27

Aumann HH, Probst RG. 1991. *Astrophys. J.* 368:264–71

Backman DE, Paresce F. 1993. In *Protostars and Planets III*, ed. EH Levy, JI Lunine, pp. 1253–1304. Tucson: Univ. Ariz. Press

Basri G, Brown ME. 2006. *Annu. Rev. Earth Planet. Sci.* 34:193–216

Beckwith SVW, Henning T, Nakagawa Y. 2000. In *Protostars and Planets IV*, ed. V Mannings, AP Boss, SS Russell, pp. 533–58. Tucson: Univ. Ariz. Press

Beichman CA, Bryden G, Gautier TN, Stapelfeldt KR, Werner MW, et al. 2005. *Astrophys. J.* 626:1061–1069

Beichman CA, Bryden G, Stapelfeldt KR, Gautier TN, Grogan K, et al. 2006a. *Astrophys. J.* 652:1674–93

Beichman CA, Tanner A, Bryden G, Stapelfeldt KR, Werner MW, et al. 2006b. *Astrophys. J.* 639:1166–76

Benedict GF, McArthur B, Gatewood G, Nelan E, Cochran W, et al. 2006. *Astron. J.* 132:2206–18

Besla G, Wu Y. 2007. *Astrophys. J.* 655:528–40

Beust H, Morbidelli A. 2000. *Icarus* 143:170–88

Beust H, Valiron P. 2007. *Astron. Astrophys.* 466:201–13

Bonfils X, Mayor M, Delfosse X, Forveille T, Gillon M, et al. 2007. *Astron. Astrophys.* 474:293–99

Bottke WF, Durda DD, Nesvorný D, Jedicke R, Morbidelli A, et al. 2005. *Icarus* 175:111–40

Bottke WF, Levison HF, Nesvorný D, Dones L. 2007. *Icarus* 190:203–23

Brandeker A, Liseau R, Olofsson G, Fridlund M. 2004. *Astron. Astrophys.* 413:681–91

Bryden G, Beichman CA, Trilling DE, Rieke GH, Holmes EK, et al. 2006. *Astrophys. J.* 636:1098–113

Calvet N, Briceño C, Hernández J, Hoyer S, Hartmann L, et al. 2005a. *Astron. J.* 129:935–46

Calvet N, D'Alessio P, Watson DM, Franco-Hernańdez R, Furlan E, et al. 2005b. *Astrophys. J.* 630:L185–88

Canup RM. 2004. *Annu. Rev. Astron. Astrophys.* 42:441–75

Canup RM. 2005. *Science* 307:546–50

Carpenter JM, Mamajek EE, Hillenbrand LA, Meyer MR. 2006. *Astrophys. J.* 651:L49–52

Chambers JE, Wetherill GW. 1998. *Icarus* 136:304–27

Chen CH, Jura M. 2001. *Astrophys. J.* 560:L171–74

Chen CH, Jura M, Gordon KD, Blaylock M. 2005. *Astrophys. J.* 623:493–501

Chen CH, Kamp I. 2004. *Astrophys. J.* 602:985–92

Chen CH, Li A, Bohac C, Kim KH, Watson DM, et al. 2007. *Astrophys. J.* 666:466–74

Chen CH, Sargent BA, Bohac C, Kim KH, Leibensperger E, et al. 2006. *Astrophys. J. Suppl. Ser.* 166:351–77

Chiang EI, Lithwick Y, Murray-Clay R, Buie M, Grundy W, Holman M. 2007. See Reipurth et al 2007, pp. 895–911

Cieza L, Padgett DL, Stapelfeldt KR, Augereau J-C, Harvey P, et al. 2007. *Astrophys. J.* 667:308–28

Clampin M, Krist JE, Ardila DR, Golimowski DA, Hartig GF, et al. 2003. *Astron. J.* 126:385–92

Clarke CJ, Gendrin A, Sotomayor M. 2001. *MNRAS* 328:485–91

Currie T, Kenyon S, Balog Z, Rieke G, Bragg A, Bromley B. 2008. *Astrophys. J.* 672:558–74

Czechowski A, Mann I. 2007. *Astrophys. J.* 660:1541–55

Decin G, Dominik C, Waters LBFM, Waelkens C. 2003. *Astrophys. J.* 598:636–44

Dent WRF, Greaves JS, Coulson IM. 2005. *MNRAS* 359:663–76

Dermott SF, Grogan K, Durda DD, Jayaraman S, Kehoe TJJ, et al. 2001. In *Interplanetary Dust*, ed. E Grun, BAS Gustafson, SF Dermott, H Fechtig, pp. 569–639. Berlin: Springer-Verlag

di Folco E, Absil O, Augereau J-C, Mérand A, Coudé du Foresto V, et al. 2007. *Astron. Astrophys.* 475:243–50

Dominik C, Blum J, Cuzzi JN, Wurm G. 2007. See Reipurth et al. 2007, pp. 783–800

Dominik C, Decin G. 2003. *Astrophys. J.* 598:626–35

Dullemond CP, Dominik C. 2005. *Astron. Astrophys.* 434:971–86

Dullemond CP, Hollenbach DE, Kamp I, D'Alessio P. 2007. See Reipurth et al. 2007, pp. 555–72

Durda DD, Greenberg R, Jedicke R. 1998. *Icarus* 135:431–40

Durisen RH, Boss AP, Mayer L, Nelson AF, Quinn T, Rice WKM. 2007. See Reipurth et al. 2007, pp. 607–22

Faber P, Quillen AC. 2007. *MNRAS* 382:1823–28

Farley KA, Vokrouhlický D, Bottke WF, Nesvorný D. 2006. *Nature* 439:295–97

Fernández JA, Ip WH. 1984. *Icarus* 58:109–120

Fernández R, Brandeker A, Wu Y. 2006. *Astrophys. J.* 643:509–22

Fisher RS, Telesco CM, Piña RK, Knacke RF, Wyatt MC. 2000. *Astrophys. J.* 532:L141–44

Fitzgerald MP, Kalas PG, Duchene G, Pinte C, Graham JR. 2007. *Astrophys. J.* 670:536–56

Ford EB, Chiang EI. 2007. *Astrophys. J.* 661:602–15

Ford EB, Rasio FA. 2007. *Ap. J.* In press

Freistetter F, Krivov AV, Löhne T. 2007. *Astron. Astrophys.* 466:389–93

Gaidos EJ. 1999. *Astrophys. J.* 510:L131–34

Garaud P. 2007. *Astrophys. J.* 671:2091–2114

Gáspár A, Su KYL, Rieke GH, Balog Z, Kamp I, et al. 2008. *Astrophys. J.* 672:974–83

Gautier TN III, Rieke GH, Stansberry J, Bryden GC, Stapelfeldt KR, et al. 2007. *Astrophys. J.* 667:527–36

Goldreich P, Lithwick Y, Sari R. 2004a. *Annu. Rev. Astron. Astrophys.* 42:549–601

Goldreich P, Lithwick Y, Sari R. 2004b. *Astrophys. J.* 614:497–507

Gomes R, Levison HF, Tsiganis K, Morbidelli A. 2005. *Nature* 435:466–69

Gomes RS, Morbidelli A, Levison HF. 2004. *Icarus* 170:492–507

Gorlova N, Rieke GH, Muzerolle J, Stauffer JR, Siegler N, et al. 2006. *Astrophys. J.* 649:1028–1042

Greaves JS, Fischer DA, Wyatt MC. 2006. *MNRAS* 366:283–86

Greaves JS, Holland WS, Jayawardhana R, Wyatt MC, Dent WRF. 2004a. *MNRAS* 348:1097–104

Greaves JS, Holland WS, Wyatt MC, Dent WRF, Robson EI, et al. 2005. *Astrophys. J.* 619:L187–90

Greaves JS, Wyatt MC. 2003. *MNRAS* 345:1212–22

Greaves JS, Wyatt MC, Holland WS, Dent WRF. 2004b. *MNRAS* 351:L54–58

Grigorieva A, Artymowicz P, Thébault P. 2007. *Astron. Astrophys.* 461:537–49

Habing HJ, Dominik C, Jourdain de Muizon M, Laureijs RJ, Kessler MF, et al. 2001. *Astron. Astrophys.* 365:545–61

Hahn JM, Malhotra R. 1999. *Astron. J.* 117:3041–53

Haisch KE, Lada EA, Lada CJ. 2001. *Astrophys. J.* 553:L153–56

Halliday AN, Kleine T. 2006. In *Meteorites and the Early Solar System II*, ed. DS Lauretta, HY McSween Jr, pp. 775–801. Tucson: Univ. Ariz. Press

Hartmann WK, Ryder G, Dones L, Grinspoon D. 2000. In *Origin of the Earth and Moon*, ed. RM Canup, K Righter, pp. 493–512. Tucson: Univ. Ariz. Press

Heap SR, Lindler DJ, Lanz TM, Cornett RH, Hubeny I, et al. 2000. *Astrophys. J.* 539:435–44

Hernández J, Briceño C, Calvet N, Hartmann L, Muzerolle J, Quintero A. 2006. *Astrophys. J.* 652:472–81

Hernández J, Calvet N, Briceño C, Hartmann L, Vivas AK, et al. 2007a. *Astrophys. J.* 671:1784–99

Hernández J, Hartmann L, Megeath T, Gutermuth R, Muzerolle J, et al. 2007b. *Astrophys. J.* 662:1067–1081

Herrmann F, Krivov AV. 2007. *Astron. Astrophys.* 476:829–39

Hillenbrand LA, Carpenter JM, Kim JS, Meyer MR, Backman DE, et al. 2008. *Astrophys. J.* 677:630–56

Hines DC, Backman DE, Bouwman J, Hillenbrand LA, Carpenter JM, et al. 2006. *Astrophys. J.* 638:1070–79

Hines DC, Schneider G, Hollenbach D, Mamajek EE, Hillenbrand LA, et al. 2007. *Astrophys. J.* 671:L165–68

Hinz PM, Heinze AN, Sivanandam S, Miller DL, Kenworthy MA, et al. 2006. *Astrophys. J.* 653:1486–92

Holland WS, Greaves JS, Zuckerman B, Webb RA, McCarthy C, et al. 1998. *Nature* 392:788–91

Hubickyj O, Bodenheimer P, Lissauer JJ. 2005. *Icarus* 179:415–31

Huenemoerder DP, Kastner JH, Testa P, Schulz NS, Weintraub DA. 2007. *Astrophys. J.* 671:592–604

Ipatov SI, Kutyrev AS, Madsen GJ, Mather JC, Moseley SH, Reynolds RJ. 2008. *Icarus* 194:769–88

Johansen A, Oishi J, Low MM, Klahr H, Henning T, Youdin A. 2007. *Nature* 448:1022–25

Johnson JA, Butler RP, Marcy GW, Fischer DA, Vogt SS, et al. 2007. *Astrophys. J.* 670:833–40

Jonkheid B, Kamp I, Augereau JC, van Dishoeck EF. 2006. *Astron. Astrophys.* 453:163–71

Jura M. 2004. *Astrophys. J.* 603:729–37

Jura M, Malkan M, White R, Telesco C, Piña R, Fisher RS. 1998. *Astrophys. J.* 505:897–902

Juric M, Tremaine S. 2008. *Ap. J.* In press

Kalas P. 2005. *Astrophys. J.* 635:L169–72

Kalas P, Duchene G, Fitzgerald MP, Graham JR. 2007. *Astrophys. J.* 671:L161–64

Kalas P, Fitzgerald MP, Graham JR. 2007. *Astrophys. J.* 661:L85–88

Kalas P, Graham JR, Beckwith SVW, Jewitt DC, Lloyd JP. 2002. *Astrophys. J.* 567:999–1012

Kalas P, Graham JR, Clampin M. 2005. *Nature* 435:1067–1070

Kalas P, Graham JR, Clampin MC, Fitzgerald MP. 2006. *Astrophys. J.* 637:L57–60

Kenyon SJ, Bromley BC. 2002. *Astron. J.* 123:1757–75

Kenyon SJ, Bromley BC. 2004a. *Astron. J.* 127:513–30

Kenyon SJ, Bromley BC. 2004b. *Astrophys. J.* 602:L133–36

Kenyon SJ, Bromley BC. 2005. *Astron. J.* 130:269–79

Kenyon SJ, Bromley BC. 2006. *Astron. J.* 131:1837–50

Klahr H, Lin DNC. 2001. *Astrophys. J.* 554:1095–1109

Klahr H, Lin DNC. 2005. *Astrophys. J.* 632:1113–21

Kokubo E, Ida S. 1998. *Icarus* 131:171–78

Kortenkamp SJ, Dermott SF. 1998. *Icarus* 135:469–95

Krivov AV, Löhne T, Sremcević M. 2006. *Astron. Astrophys.* 455:509–19

Krivov AV, Queck M, Löhne T, Sremcević M. 2007. *Astron. Astrophys.* 462:199–210

Kuchner MJ, Holman MJ. 2003. *Astrophys. J.* 588:1110–20

Lada CJ, Muench AA, Luhman KL, Allen L, Hartmann L, et al. 2006. *Astron. J.* 131:1574–1607
Lagrange AM, Backman DE, Artymowicz P. 2000. In *Protostars and Planets IV*, ed. V Mannings, AP Boss, SS Russell, pp. 639–72. Tucson: Univ. Ariz. Press
Larwood JD, Kalas PG. 2001. *MNRAS* 323:402–16
Laureijs RJ, Jourdain de Muizon M, Leech K, Siebenmorgen R, Dominik C, et al. 2002. *Astron. Astrophys.* 387:285–93
Lecar M, Franklin FA, Holman MJ, Murray NJ. 2001. *Annu. Rev. Astron. Astrophys.* 39:581–631
Leinhardt ZM, Richardson DC. 2005. *Astrophys. J.* 625:427–40
Lestrade JF, Wyatt MC, Bertoldi F, Dent WRF, Menten KM. 2006. *Astron. Astrophys.* 460:733–41
Levison HF, Morbidelli A, Dones L. 2004. *Astron. J.* 128:2553–63
Levison HF, Morbidelli A, Gomes R, Backman DE. 2007. See Reipurth et al. 2007, pp. 669–84
Liou JC, Zook HA. 1999. *Astron. J.* 118:580–90
Lissauer JJ. 1993. *Annu. Rev. Astron. Astrophys.* 31:129–74
Lisse C, Schultz A, Fernandez Y, Peschke S, Ressler M, et al. 2002. *Astrophys. J.* 570:779–84
Lisse CM, Beichman CA, Bryden G, Wyatt MC. 2007. *Astrophys. J.* 658:584–92
Lisse CM, Chen C, Wyatt MC, Morlok A. 2008. *Astrophys. J.* 673:1106–22
Liu MC, Matthews BC, Williams JP, Kalas PG. 2004. *Astrophys. J.* 608:526–32
Löhne T, Krivov AV, Rodmann J. 2008. *Astrophys. J.* 673:1123–37
Lovis C, Mayor M, Pepe F, Alibert Y, Benz W, et al. 2006. *Nature* 441:305–9
Low FJ, Smith PS, Werner M, Chen C, Krause V, et al. 2005. *Astrophys. J.* 631:1170–79
Low FJ, Young E, Beintema DA, Gautier TN, Beichman CA, et al. 1984. *Astrophys. J.* 278:L19–22
Mamajek EE, Meyer MR. 2007. *Astrophys. J.* 668:L175–78
Mann I, Köhler M, Kimura H, Czechowski A, Minato T. 2006. *Astron. Astrophys. Rev.* 13:159–228
Mannings V, Barlow MJ. 1998. *Astrophys. J.* 497:330–41
Mannings V, Sargent AI. 1997. *Astrophys. J.* 490:792–802
Martin RG, Lubow SH, Pringle JE, Wyatt MC. 2007. *MNRAS* 378:1589–1600
Matthews BC, Kalas PG, Wyatt MC. 2007. *Astrophys. J.* 663:1103–9
Matthews BC, Greaves JS, Holland WS, Wyatt MC, Barlow MJ, et al. 2007. *Publ. Astron. Soc. Pac.* 119:842–54
McCabe C, Ghez AM, Prato L, Duchene G, Fisher RS, Telesco C. 2006. *Astrophys. J.* 636:932–51
Megeath ST, Hartmann L, Luhman KL, Fazio GG. 2005. *Astrophys. J.* 634:L113–16
Meyer MR, Backman DE, Weinberger AJ, Wyatt MC. 2007. See Reipurth et al. 2007, pp. 573–88
Meyer MR, Carpenter JM, Mamajek EE, Hillenbrand LA, Hollenbach D, et al. 2008. *Astrophys. J.* 673:L181–84
Moerchen MM, Telesco CM, De Buizer JM, Packham C, Radomski JT. 2007a. *Astrophys. J.* 666:L109–12
Moerchen MM, Telesco CM, Packham C, Kehoe TJJ. 2007b. *Astrophys. J.* 655:L109–12
Moór A, Ábrahám P, Derekas A, Kiss C, Kiss LL, et al. 2006. *Astrophys. J.* 644:525–42
Morbidelli A, Levison HF, Gomes R. 2008. In *The Solar System Beyond Neptune*, ed. A Barucci, H Boehnhardt, D Cruikshank, A Morbidelli, pp. 275–92. Tucson: Univ. Ariz. Press
Morbidelli A, Levison HF, Tsiganis K, Gomes R. 2005. *Nature* 435:462–65
Moro-Martín A, Malhotra R. 2002. *Astron. J.* 124:2305–21
Moro-Martín A, Malhotra R, Carpenter JM, Hillenbrand LA, Wolf S, et al. 2007. *Astrophys. J.* 668:1165–73
Moro-Martín A, Wyatt MC, Malhotra R, Trilling DE. 2008. In *The Solar System Beyond Neptune*, ed. A Barucci, H Boehnhardt, D Cruikshank, A Morbidelli, pp. 465–80. Tucson: Univ. Ariz. Press.
Najita J, Williams JP. 2005. *Astrophys. J.* 635:625–35
Natta A, Testi L, Calvet N, Henning T, Waters R, Wilner D. 2007. See Reipurth et al. 2007, pp. 767–81
Nesvorný D, Bottke WF, Levison HF, Dones L. 2003. *Astrophys. J.* 591:486–97
O'Brien DP, Greenberg R. 2003. *Icarus* 164:334–45
O'Brien DP, Morbidelli A, Bottke WF. 2007. *Icarus* 191:434–52
Oudmaijer RD, van der Veen WECJ, Waters LBFM, Trams NR, Waelkens C, Engelsman E. 1992. *Astron. Astrophys. Suppl. Ser.* 96:625–43
Ozernoy LM, Gorkavyi NN, Mather JC, Taidakova TA. 2000. *Astrophys. J.* 537:L147–51
Padgett DL, Cieza L, Stapelfeldt KR, Evans NJ, Koerner D, et al. 2006. *Astrophys. J.* 645:1283–96

Papaloizou JCB, Nelson RP, Kley W, Masset FS, Artymowicz P. 2007. See Reipurth et al. 2007, pp. 655–68

Papaloizou JCB, Terquem C. 2006. *Rep. Prog. Phys.* 69:119–80

Pascucci I, Gorti U, Hollenbach D, Najita J, Meyer MR, et al. 2006. *Astrophys. J.* 651:1177–93

Plavchan P, Jura M, Lipsky SJ. 2005. *Astrophys. J.* 631:1161–69

Poulton CJ, Greaves JS, Cameron AC. 2006. *MNRAS* 372:53–59

Quillen AC. 2006. *MNRAS* 372:L14–18

Quillen AC, Blackman EG, Frank A, Varniere P. 2004. *Astrophys. J.* 612:L137–40

Quillen AC, Morbidelli A, Moore A. 2007. *MNRAS* 380:1642–48

Reche R, Beust H, Augereau JC, Absil O. 2008. *Astron. Astrophys.* 480:551–61

Redfield S. 2007. *Astrophys. J.* 656:L97–100

Reipurth B, Jewitt D, Keil K, eds. 2007. *Protostars and Planets V.* Tucson: Univ. Ariz. Press

Rhee JH, Song I, Zuckerman B. 2008. *Astrophys. J.* 675:777–83

Rhee JH, Song I, Zuckerman B, McElwain M. 2007. *Astrophys. J.* 660:1556–71

Rieke GH, Su KYL, Stansberry JA, Trilling D, Bryden G, et al. 2005. *Astrophys. J.* 620:1010–1026

Roberge A, Feldman PD, Weinberger AJ, Deleuil M, Bouret JC. 2006. *Nature* 441:724–26

Scally A, Clarke C. 2001. *MNRAS* 325:449–56

Schneider G, Silverstone MD, Hines DC, Augereau J-C, Pinte C, et al. 2006. *Astrophys. J.* 650:414–31

Scholz A, Jayawardhana R, Wood K, Meeus G, Stelzer B, et al. 2007. *Astrophys. J.* 660:1517–31

Sheret I, Dent WRF, Wyatt MC. 2004. *MNRAS* 348:1282–94

Sicilia-Aguilar A, Hartmann L, Calvet N, Megeath ST, Muzerolle J, et al. 2006. *Astrophys. J.* 638:897–919

Siegler N, Muzerolle J, Young ET, Rieke GH, Mamajek EE, et al. 2007. *Astrophys. J.* 654:580–94

Smith BA, Terrile RJ. 1984. *Science* 226:1421–24

Smith R, Wyatt MC, Dent WRF. 2008. *Astron. Astrophys.* In press

Song I, Weinberger AJ, Becklin EE, Zuckerman B, Chen C. 2002. *Astron. J.* 124:514–18

Song I, Zuckerman B, Weinberger AJ, Becklin EE. 2005. *Nature* 436:363–65

Spangler C, Sargent AI, Silverstone MD, Becklin EE, Zuckerman B. 2001. *Astrophys. J.* 555:932–44

Stapelfeldt KR, Holmes E, Chen C, Rieke G, Su K, et al. 2004. *Astrophys. J. Suppl. Ser.* 154:458–62

Stauffer JR, Rebull LM, Carpenter J, Hillenbrand L, Backman D, et al. 2005. *Astron. J.* 130:1834–44

Stern SA. 1996. *Astron. J.* 112:1203–11

Strom RG, Malhotra R, Ito T, Yoshida F, Kring DA. 2005. *Science* 309:1847–50

Strubbe LE, Chiang EI. 2006. *Astrophys. J.* 648:652–65

Su KYL, Rieke GH, Misselt KA, Stansberry JA, Moro-Martin A, et al. 2005. *Astrophys. J.* 628:487–500

Su KYL, Rieke GH, Stansberry JA, Bryden G, Stapelfeldt KR, et al. 2006. *Astrophys. J.* 653:675–89

Sykes MV, Lebofsky LA, Hunten DM, Low F. 1986. *Science* 232:1115–17

Takeda G, Ford EB, Sills A, Rasio FA, Fischer DA, Valenti JA. 2007. *Astrophys. J. Suppl. Ser.* 168:297–318

Takeuchi T, Artymowicz P. 2001. *Astrophys. J.* 557:990–1006

Tanaka H, Inaba S, Nakazawa K. 1996. *Icarus* 123:450–55

Telesco CM, Fisher R, Pia R, Knacke R, Dermott S, et al. 2000. *Astrophys. J.* 530:329–41

Telesco CM, Fisher R, Wyatt M, Dermott S, Kehoe T, et al. 2005. *Nature* 433:133–36

Thébault P, Augereau JC. 2007. *Astron. Astrophys.* 472:169–85

Thébault P, Augereau JC, Beust H. 2003. *Astron. Astrophys.* 472:169–85

Thébault P, Marzari F, Scholl H. 2006. *Icarus* 183:193–206

Thébault P, Wu Y. 2008. *Astron. Astrophys.* 481:713–24

Thommes EW, Bryden G, Wu Y, Rasio FA. 2007. *Astrophys. J.* 675:1538–48

Thommes EW, Duncan MJ, Levison HF. 1999. *Nature* 402:635–38

Throop HB, Bally J. 2005. *Astrophys. J.* 623:L149–52

Trilling DE, Bryden G, Beichman CA, Rieke GH, Su KYL, et al. 2008. *Astrophys. J.* 674:1086–105

Tsiganis K, Gomes R, Morbidelli A, Levison HF. 2005. *Nature* 435:459–61

Udry S, Santos NC. 2007. *Annu. Rev. Astron. Astrophys.* 45:397–439

Uzpen B, Kobulnicky HA, Monson AJ, Pierce MJ, Clemens DP, et al. 2007. *Astrophys. J.* 658:1264–88

Wahhaj Z, Koerner DW, Sargent AI. 2007. *Astrophys. J.* 661:368–73

Werner MW, Roellig TL, Low FJ, Rieke GH, Rieke M, et al. 2004. *Astrophys. J. Suppl. Ser.* 154:1–9

Wetherill GW, Stewart GR. 1989. *Icarus* 77:330–57

Williams JP, Andrews SM. 2006. *Astrophys. J.* 653:1480–85

Wood BE, Müller HR, Zank GP, Linsky JL. 2002. *Astrophys. J.* 574:412–25

Wyatt MC. 2003. *Astrophys. J.* 598:1321–40

Wyatt MC. 2005a. *Astron. Astrophys.* 433:1007–1012

Wyatt MC. 2005b. *Astron. Astrophys.* 440:937–48

Wyatt MC. 2006. *Astrophys. J.* 639:1153–65

Wyatt MC. 2008. In *Small Bodies in Planetary Systems*, ed. I Mann, AM Nakamura, T Mukai. Heidelberg: Springer-Verlag GmbH. In press

Wyatt MC, Clarke CJ, Greaves JS. 2007. *MNRAS* 380:1737–43

Wyatt MC, Dent WRF. 2002. *MNRAS* 334:589–607

Wyatt MC, Dent WRF, Greaves JS. 2003. *MNRAS* 342:876–88

Wyatt MC, Dermott SF, Telesco CM, Fisher RS, Grogan K, et al. 1999. *Astrophys. J.* 527:918–44

Wyatt MC, Greaves JS, Dent WRF, Coulson IM. 2005. *Astrophys. J.* 620:492–500

Wyatt MC, Smith R, Beichman CA, Bryden G, Greaves JS, Lisse CM. 2007a. *Astrophys. J.* 658:569–83

Wyatt MC, Smith R, Su KYL, Rieke GH, Greaves JS, et al. 2007b. *Astrophys. J.* 663:365–82

Youdin AN, Shu FH. 2002. *Astrophys. J.* 580:494–505

Young ET, Lada CJ, Teixeira P, Muzerolle J, Muench A, et al. 2004. *Astrophys. J. Suppl. Ser.* 154:428–32

Zuckerman B. 2001. *Annu. Rev. Astron. Astrophys.* 39:549–80

Zuckerman B, Becklin EE. 1993. *Astrophys. J.* 414:793–802

Zuckerman B, Song I. 2004. *Annu. Rev. Astron. Astrophys.* 42:685–721

Contents

Indexes

Errata

An online log of corrections to *Annual Review of Astronomy and Astrophysics* articles may
be found at http://astro.annualreviews.org/errata.shtml